T.C.
REPUBLIC OF TURKEY
HACETTEPE UNIVERSITY
GRADUATE SCHOOL OF HEALTH SCIENCES

THE RELATION BETWEEN HUMAN COCHLEAR DUCT LENGTH AND HEAD SIZE ASSESSED BY MRI AND CBCT

İrem ADALILAR (Audiologist)

Program of Audiology
MASTER OF SCIENCE THESIS

ANKARA
2022

T.C.
REPUBLIC OF TURKEY
HACETTEPE UNIVERSITY
GRADUATE SCHOOL OF HEALTH SCIENCES

THE RELATION BETWEEN HUMAN COCHLEAR DUCT LENGTH AND HEAD SIZE ASSESSED BY MRI AND CBCT

İrem ADALILAR (Audiologist)

Program of Audiology
MASTER OF SCIENCE THESIS

ADVISOR OF THE THESIS
Asst. Prof. Dr. Hilal DİNÇER D'ALESSANDRO

CO-ADVISOR OF THE THESIS
Prof. Dr. Andrej KRAL

ANKARA
2022

HACETTEPE UNIVERSITY
GRADUATE SCHOOL OF HEALTH SCIENCES

THE RELATION BETWEEN HUMAN COCHLEAR DUCT LENGTH AND HEAD SIZE ASSESSED BY MRI AND CBCT

İrem ADALILAR

Advisor: Asst. Prof. Dr. Hilal DİNÇER D'ALESSANDRO

Co-Advisor: Prof. Dr. Andrej KRAL

This thesis study has been approved and accepted as a Master dissertation in "Audiology Program" by the assessment committee, whose members are listed below, on 27.04.2022.

Chairman of the Committee:	*Prof. Dr. Gonca SENNAROĞLU* *Hacettepe University*	(Signature)
Advisor of the Dissertation:	*Asst.Prof.Dr. Hilal DİNÇER D'ALESSANDRO* *Hacettepe University*	(Signature)
Member:	*Prof.Dr. Levent SENNAROĞLU* *Hacettepe University*	(Signature)
Member:	*Assoc.Prof.Dr. Didem TÜRKYILMAZ* *Hacettepe University*	(Signature)
Member:	*Asst.Prof.Dr. Asuman ALNIAÇIK* *Başkent University*	(Signature)

This dissertation has been approved by the above committee in conformity to the related issues of Hacettepe University Graduate Education and Examination Regulation.

Prof. Müge YEMİŞÇİ ÖZKAN, MD, PhD

Director

YAYIMLAMA VE FİKRİ MÜLKİYET HAKLARI BEYANI

Enstitü tarafından onaylanan lisansüstü tezimin/raporumun tamamını veya herhangi bir kısmını, basılı (kağıt) ve elektronik formatta arşivleme ve aşağıda verilen koşullarla kullanıma açma iznini Hacettepe Üniversitesine verdiğimi bildiririm. Bu izinle Üniversiteye verilen kullanım hakları dışındaki tüm fikri mülkiyet haklarım bende kalacak, tezimin tamamının ya da bir bölümünün gelecekteki çalışmalarda (makale, kitap, lisans ve patent vb.) kullanım hakları
bana ait olacaktır.

Tezin kendi orijinal çalışmam olduğunu, başkalarının haklarını ihlal etmediğimi ve tezimin tek yetkili sahibi olduğumu beyan ve taahhüt ederim. Tezimde yer alan telif hakkı bulunan ve sahiplerinden yazılı izin alınarak kullanılması zorunlu metinlerin yazılı izin alınarak kullandığımı ve istenildiğinde suretlerini Üniversiteye teslim etmeyi taahhüt ederim. Yüksek Öğretim Kurulu tarafından yayınlanan "**Lisansüstü Tezlerin Elektronik Ortamda Toplanması, Düzenlenmesi ve Erişime Açılmasına İlişkin Yönerge**" kapsamında tezim aşağıda belirtilen koşullar haricince YÖK Ulusal Tez Merkezi / H.Ü. Kütüphaneleri Açık Erişim Sisteminde erişime açılır.

o Enstitü / Fakülte yönetim kurulu kararı ile tezimin erişime açılması mezuniyet tarihimden itibaren 2 yıl ertelenmiştir. (1)

X Enstitü / Fakülte yönetim kurulunun gerekçeli kararı ile tezimin erişime açılması mezuniyet tarihimden itibaren 6 ay ertelenmiştir. (2)

o Tezimle ilgili gizlilik kararı verilmiştir. (3)

28/04/2022

İrem ADALILAR

1"Lisansüstü Tezlerin Elektronik Ortamda Toplanması, Düzenlenmesi ve Erişime Açılmasına İlişkin Yönerge"

*(1) Madde 6. 1. Lisansüstü tezle ilgili patent başvurusu yapılması veya patent alma sürecinin devam etmesi durumunda, tez **danışmanının** önerisi ve **enstitü anabilim dalının** uygun görüşü üzerine **enstitü** veya **fakülte yönetim kurulu** iki yıl süre ile tezin erişime açlmasının ertelenmesine karar verebilir.*

*(2) Madde 6. 2. Yeni teknik, materyal ve metotların kullanıldığı, henüz makaleye dönüşmemiş veya patent gibi yöntemlerle korunmamış ve internetten paylaşılması durumunda 3. şahıslara veya kurumlara haksız kazanç imkanı oluşturabilecek bilgi ve bulguları içeren tezler hakkında tez **danışmanının** önerisi ve **enstitü anabilim dalının** uygun görüşü üzerine **enstitü** veya **fakülte yönetim kurulunun** gerekçeli kararı ile altı ayı aşmamak üzere tezin erişime açılması engellenebilir.*

*(3) Madde 7. 1. Ulusal çıkarları veya güvenliği ilgilendiren, emniyet, istihbarat, savunma ve güvenlik, sağlık vb.konulara ilişkin lisansüstü tezlerle ilgili gizlilik kararı, **tezin yapıldığı kurum** tarafından verilir *. Kurum ve kuruluşlarla yapılan işbirliği protokolü çerçevesinde hazırlanan lisansüstü tezlere ilişkin gizlilik kararı ise, **ilgili kurum ve kuruluşun önerisi** ile **enstitü** veya **fakültenin** uygun görüşü üzerine **üniversite yönetim kurulu** tarafından verilir. Gizlilik kararı verilen tezler Yüksek öğretim Kuruluna bildirilir.*

Madde 7.2. Gizlilik kararı verilen tezler gizlilik süresince enstitü veya fakülte tarafından gizlilik kuralları çerçevesinde muhafaza edilir, gizlilik kararının kaldırılması halinde Tez Otomasyon Sistemine yüklenir

** Tez **danışmanının** önerisi ve **enstitü anabilim dalının** uygun görüşü üzerine **enstitü** veya **fakülte yönetim kurulu tarafından karar verilir**.*

ETHICAL DECLARATION

In this thesis study, I declare that all the information and documents have been obtained in the base of the academic rules and all audio-visual and written information and results have been presented according to the rules of scientific ethics. I did not do any distortion in data set. In case of using other works, related studies have been fully cited in accordance with the scientific standards. I also declare that my thesis study is original except cited references. It was produced by myself in consultation with supervisor (The Relation Between Human Cochlear Duct Length and Head Size Assessed by MRI and CBCT, İrem ADALILAR) and written according to the rules of thesis writing of Hacettepe University Graduate School of Health Sciences.

İrem ADALILAR

ACKNOWLEDGEMENT

At the end of this wonderful 2 years adventure, I have learned “No one who achieves success able to do so without acknowledging the help of others” and I would like to thank:

My advisor who invited me to his spectacular laboratory in Germany and made my dreams come true by allowing me to do research in this environment, enlightened me at every meeting with his unlimited knowledge share, and whom I admire with his patience and humanity, Prof. Dr. Andrej KRAL.

My advisor who shared her great knowledge with me in every moment after each result and patiently supports me in all situations, Asst. Prof. Dr. Hilal DİNÇER D’ALESSANDRO.

The academician who gave me the chance to proceed with my dreams and caused me to discover my interests throughout my undergraduate and graduate life with her knowledge and care, Assoc. Prof. Dr. Meral Didem TÜRKYILMAZ.

The head of the department who gave me this opportunity and made me love my profession with her extraordinary accomplishment in audiology, Prof. Dr. Gonca SENNAROĞLU.

The scientist who listened me and supported me with his extensive knowledge in my study field, Dr. Peter HOOBKA.

Those scientists who informed me and helped me when I solved problems I had with images, Dr. Daniel SCHURZIG and Dr. Max Eike TIMM.

Those PhD students who were always with me in the laboratory and made me adapt to a new country, always with their friendly conversations and a cup of coffee, Niloofar TAVAKOLI and Lea SOLLMAN.

My family who supported me with their love and gave me strength in every decision I made materially and spiritually, my MOM and DAD.

My friend who trusted me and made me believe that I can always do better and stayed with me with his encouragement Talha ŞENER.

ABSTRACT

Adalılar, İ., The Relation Between Human Cochlear Duct Length And Head Size assessed by MRI and CBCT, Hacettepe University Graduate School of Health Sciences Audiology Department of Audiology Master of Science Thesis, Ankara, 2022. The cochlea differs in length and shape among individuals and this might be due to the fact that it is affected by spatial constraints. The head size may restrict the cochlea which is located in the temporal bone, and individuals with smaller head sizes may have shorter cochlear duct lengths (CDL). On the other hand, normal-hearing participants with longer CDLs have an increase in low-frequency sensitivity. Therefore, not only the CDL but also auditory outcomes are thought to be significantly affected by cochlear structures and the factors affecting CDL may also affect outcomes of cochlear implantation. The head in which the cochlea is located and develops together, as well as, the body height in the human body are structures that continue to grow until certain periods after birth. Despite differences in the developmental process, the cochlea, head, and height may have a genetic makeup that is interconnected and affect one another. Hence, these growing parts of the body may influence the CDL during the development process. The present study was conducted with the aim of finding any relations between mentioned structures. It consisted of a study group that contained 112 postlingual-deafened adult participants who were cochlear implant users. Cone Beam Computed Tomography (CBCT) images of the cochlea and Magnetic Resonance (MR) images of the head were performed for each participant in the present study group. CDLs were determined via CBCT, head size measures were determined by 3D conversion via MRI, and the body height was completed. In terms of CDL, head size, and height: females had smaller averages than that males. The results of this study showed that CDL had not any significant correlation with head size but a weak correlation with height. Similar to the literature, the height and the head size showed statistically significant relationships with each other. Only CDL which was measured in the cochlea, may not be sufficient to demonstrate the effect of head size on the cochlea. Future studies might look at the links between the cochlear shape and its surroundings by using micro-CT.

Key Words: Cochlear Duct Length, Cochlear Shape, Head Size, MRI, CBCT.

ÖZET

Adalılar, İ., BT VE MRG ile değerlendirilen insan koklear kanal uzunluğu ve kafa boyutu arasındaki ilişki, Hacettepe Üniversitesi Sağlık Bilimleri Enstitüsü Odyoloji Programı Yüksek Lisans Tezi, Ankara, 2022. Koklea bireyler arasında uzunluk ve şekil olarak farklılık gösterir ve bunun sebebi kokleanın uzamsal kısıtlamalardan etkilenmesi olabilir. Kafa boyutu, temporal kemikte bulunan kokleayı kısıtlayabilir ve kafa boyutu daha küçük olan bireylerin daha kısa koklear kanal uzunluğu (KKU)'na sahip olması olasıdır. Bunun dışında, daha uzun KKU'ya sahip normal işiten katılımcılar daha fazla alçak frekans duyarlılığına sahiptir. Bu nedenle, sadece KKU'nun değil, işitsel sonuçların da koklear yapılardan önemli ölçüde etkilendiği ve KKU'yu etkileyen faktörlerin koklear implantasyon sonuçlarını etkileyebileceği düşünülmektedir. Kokleanın bulunduğu ve birlikte geliştiği kafa ve vücut boy uzunluğu doğumdan sonra belirli dönemlere kadar büyümeye devam eden yapılardır. Gelişim sürecindeki farklılıklara rağmen, koklea, kafa ve vücut boy uzunluğu birbiriyle bağlantılı ve birbirini etkileyen genetik yapıya sahip olabilir. Bu nedenle, vücudun bu büyüyen kısımları, gelişim sürecinde KKU'yu etkileyebilir. Bu araştırma, bahsedilen yapılar arasındaki herhangi bir ilişkiyi bulmak amacıyla gerçekleştirilmiştir. Araştırma, koklear implant kullanıcısı olan 112 postlingual işitme kayıplı yetişkin katılımcının yer aldığı bir çalışma grubundan oluşmuştur. Çalışma grubundaki her katılımcı için kokleanın Koni Işınlı Bilgisayarlı Tomografi (BT) görüntüleri ve kafanın Manyetik Rezonans (MR) görüntüleri elde edilmiştir. Koni Işınlı BT ile belirlenen KKU, 3 boyutlu dönüştürülen MR görüntüleri ile belirlenen kafa boyutu ölçümleri ve vücut boy uzunluğu çalışmaya dahil edildi. KKU, kafa büyüklüğü ve boy varyasyonları için kadınların ortalamaları erkeklerden daha kısa bulundu. Bu çalışmanın sonuçları, KKU'nun kafa boyutu ile anlamlı bir korelasyona sahip olmadığını, ancak boy ile zayıf bir korelasyona sahip olduğunu göstermektedir. Literatürde olduğu gibi, vücut boy uzunluğu ve kafa büyüklüğü birbirleri ile istatistiksel olarak anlamlı ilişkiler göstermektedir. Kokleadan sadece KKU ölçülmüştür ve bu, kafa boyutunun koklea üzerinde etkisini göstermek için yeterli bir parametre olmayabilir. Gelecekteki çalışmalarda, mikro-BT aracılığıyla koklear şekil ve kokleayı çevreleyen yapılar arasındaki ilişkiler incelenebilir.

Anahtar Kelimeler: Koklear Kanal Uzunluğu, Koklear şekil, Kafa boyutu, MRG, BT.

TABLE OF CONTENTS

SYMBOLS AND ABBREVIATIONS

A.	Artery
ABR	Auditory Brainstem Response
AN	Auditory Nerve
BA	Broadman Area
CBCT	Cone Beam Computed Tomography
CDL	Cochlear Duct Length
CI	Cochlear Implant
CNC	Consonant-Nucleus-Consonant
CSNHL	Congenital Sensorineural Hearing Loss
CT	Computed Tomography
E	Embryonic Days
HINT	Hearing in Noise Test
HRCT	High-resolution multi-detector computed tomography
IAM	Internal Auditory Meatus
ICV	Intracranial Volume
IHCs	Inner Hair Cells
LW	Lateral Wall
MRI	Magnetic Resonance Imaging
OC	Organ of Corti
OHCs	Outer Hair Cells
ROI	Region of Interest
SSC	Semicircular Canals
TE	Time to Echo
U-HRCT	Ultra-high-resolution multi-detector computed tomography
TR	Repetition Time
WG	Weeks of Gestation

FIGURES

TABLES

1. INTRODUCTION

The human cochlea is embedded within the temporal bone's petrous section and it reaches adult size at 17-20 weeks of gestation (1,2). The cochlea is functional at birth (1,2). The scala media's length from the round window's middle to the helicotrema in the cochlea is known as the cochlear duct length (CDL) (3). Human cochlear anatomy and cochlear length have been studied for several years to investigate interindividual differences in CDL and to determine the presence of any crucial variables that may significantly affect the CDL. Indeed, CDL and cochlear shape are known to vary considerably between individuals (4–7). The cochlear apical part completes maturation later than the basal part during the early postnatal period (8). A study conducted by Avci et al. (9) reveals 3 types of cochleae, considering the scala tympani's vertical orbit. On the other hand, the number of turns of the cochlear helix, the cochlear base length, and the cochlear width varies between individuals as well (4). For millennia, the relations between form and function continue to be a hot topic of discussion (10).

Auditory outcomes are thought to be significantly affected by cochlear structures (11). Recent evidence comes from the study by Ekdale et al. (12) showing an increase in low-frequency sensitivity for normal hearing individuals with longer CDLs at the apical part. Such findings may have implications for cochlear implant (CI) electrode selection in hearing-impaired people as well. The electrode arrays of the CIs are not designed to reach the most apical areas of the cochlea, which correlate to low frequencies. Since individual variations are greater at the apical part of the cochlea, CI seeks to send frequency information at a few hundred Hertz (13). Based on the knowledge of tonotopic mapping in a normal hearing cochlea, the inability of the most apical electrodes in the electrode array to physically reach the apical regions of the cochlea is believed to result in a frequency-place mismatch. Interindividual CDL differences may further affect the amount of this mismatch and may partly explain interindividual performance differences in CI (14).

The spiral shape of the mammalian inner ear is thought to be caused by a variety of factors such as its surrounded structures and capacity to detect low-frequency sounds (4,15). A recent study by Pietsch et al. (4) suggests that the cochlea has a narrower basal width because of space restrictions around the cochlea, especially

when the facial nerve is in close vicinity to the modiolar axis. The jugular vein, internal carotid A., tensor tympani muscle, and facial nerves surround the cochlea.

During the maturational process, spatial restrictions around the cochlea may significantly impact its shape (4), thus it is reasonable to suggest that the CDL might be significantly related to head size. Subjects with small head sizes may have smaller cochleas i.e., shorter CDLs (9). Gender differences in CDLs and head size may support this notion, with females having shorter CDLs and lower head sizes than males (16). Such gender differences may partly stem from the effects of spatial constraints surrounding the cochlea. On the other hand, head size is known to be linked to a height which is another growing part of the human body (17,18). Thus, height might be another measure having significant associations with CDL.

Unlike the cochlea, the skull continues to grow in different stages and forms after birth (9,19). Similarly, height continues to increase until about the age of 20, with gender differences (20). Certainly, many factors such as nutrition significantly affect these growing parts of the body, however, the main factor is well known to be the genetic makeup of an individual. Despite differences in developmental stages, cochlea, head, and height may share interrelated genetic makeup and show significant similarities in size (21).

To the best of our knowledge, the present study is the first attempt to investigate the relations between CDL with the two growing parts of the body: head size and height. For this purpose, human CDLs and head size assessed Cone Beam Computed Tomography (CBCT) and Magnetic Resonance Imaging (MRI), respectively. Here, instead of the traditional head circumference method, a 3D conversion of MRI is used to measure the linear lengths between certain reference points on the head and in the skull. MRI might be another reliable tool to measure the head size, due to the ability to flexibly zoom and feasibility (22).

The study is believed to provide insights into understanding anatomic and physiological variances in human cochlea, head size, and height. The study hypotheses are given below.

Hypothesis 1

H0: There are no statistically significant positive correlations between CDL and the head size of individuals.

H1: There are statistically significant positive correlations between CDL and the head size of individuals.

Hypothesis 2

H0: There are no statistically significant positive correlations between CDL and the height of individuals.

H1: There are statistically significant positive correlations between CDL and the height of individuals.

2. GENERAL INFORMATION

2.1. Introduction to the Auditory System

The outer (external) ear, middle ear, and inner ear are the three sections of the auditory system. Sounds enter through the external ear, pass through the middle ear, and finally reach the inner ear, as well as the periphery and central auditory system routes.

2.1.1. External and Middle Ear Anatomy

The external ear is one of the defining features of the head. It mainly consists of the helix, lobule, triangular fossa, external auditory canal, tympanic membrane, and eustachian tube. The middle ear starts with the tympanic membrane and consists of the incus, malleus, stapes which are the human body's smallest bones, and the Eustachian tube which unites the middle ear cavity to the pharynx.

The external auditory canal is a 3 cm S-shaped tunnel with a 0.6 cm average diameter. The ear canal's external third is cartilaginous, conversely, the canal's inner two-thirds are osseous., with the temporal bone tympanic part forming the canal's wall (1). The middle ear is a hollow, air-filled area within the temporal bone, and the size of the middle-ear cavities varies considerably from person to person (23). The oval and round windows in the middle ear's medial wall, which are part of the temporal bone, facilitate the connection between the outer and the inner ear. Other elements in the two middle ear muscles' tendons and a branch of the facial nerve that enters the cavity of the middle ear are among the other structures in the middle ear (23).

2.1.2. Temporal Bone

The temporal bone houses the cochlea, as well as the outer and the middle ear, vestibular system, and seventh and eighth cranial nerves (see figure 2.1.). The inner ear is set in the temporal bone's petrous section (1). The temporal bone is a hard, rigid bone that houses a labyrinth of chambers and canals within the skull and serves the hearing and balancing end organs; consequently, the name "labyrinth" is used to specify the bone structure (24). The temporal bone's four main segments are the mastoid (posterior to the pinna), squamous (superior to the ear canal), tympanic (ear

canal), and petrous (deep in the skull containing the inner ear). The petrous segment houses the middle ear structures, cochlea, vestibular components, and internal auditory meatus (IAM). The facial, auditory, and vestibular nerves are all located in the IAM (24). The temporal bone's petrous portion preserves the majority of the hearing mechanisms (1). The IAM opens between the base and the tip of the petrous bone. When facing the IAM's entrance, the facial nerve is at the upper left section, the auditory nerve is directly inferior to the facial nerve, and the vestibular nerves run parallel to the facial and auditory nerves (1).

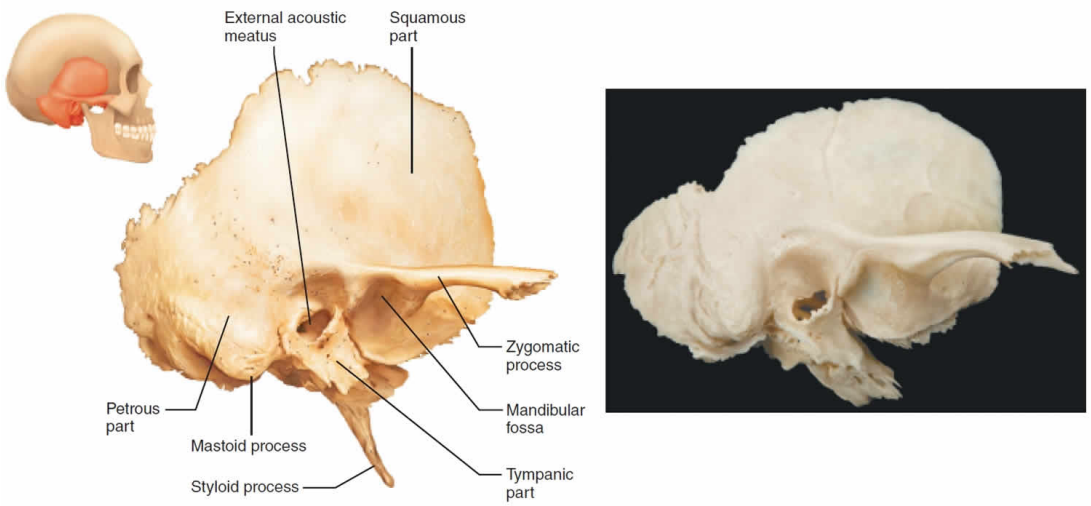

Figure 2.1. The temporal bone's lateral view and the position in the skull. The temporal bone is a hard, rigid bone that includes a labyrinth of chambers and canals within the skull. Squamous, petrous, mastoid, and tympanic are the four parts. The image has been received from the website: https://healthjade.net/temporal-bone/.

2.1.3. Inner Ear

The inner ear is a part of the ear that contains the cochlea and vestibular end organs which are composed of bony walls and form fluid canals that connect with the neural structures.

The cochlea

The cochlea in the head has an anterior and lateral apex that points toward the cheekbone. The cochlea is 30-35 mm long and measures around 0.5 cm in height in humans (23), however it can change among individuals (6,9,25–27).

The cochlea has channels with fluid in them: the scala vestibuli; the scala tympani; and the scala media (cochlear duct). The bony cochlea contains two windows,

the oval window which goes into scala vestibuli, and the round window which goes into scala tympani, that interact with the middle ear. The scala media separates the scala tympani and vestibuli, while the two outer scales interact at the apex via a tiny aperture known as the helicotrema (24).

The cochlear modiolus, which is surrounded by spiral ganglions (cell bodies of afferent neurons) and is perforated by branching chambers, covers the cochlea's 1.6–2.0 turns (1). It varies between individuals depending on the variability of the cochlear size (9). The membranous duct contains the sensory epithelium of the auditory system. The cochlea's apical end is narrower than the cochlea's base (24).

The sensory cells (hair cells) of the organ of Corti (OC) transform the vibrations of the basilar membrane into a neural code, which runs parallel to the basilar membrane and classifies sounds depending on their frequency (23). While the complex structure of the cochlea has been well-known for a long time, the relationship between its anatomy and function has remained a mystery.

Organ of Corti

The OC which is called the hearing organ (28). OC has sensory cells that consist of the inner hair cells (IHCs) and the outer hair cells (OHCs), reticular lamina, tectorial membrane, Deiter, Hensen, and Claudian cells, and habenula perforate. In humans, a single line of around 3,500 IHCs spans the cochlea and forms a flattened "U" shape with three to five lines of around 12,000 OHCs in a "W" form that also cover the cochlea (28). Cross-links on the sides of the cilia help the cilia move in synchrony when they are triggered (7). When the OHCs cilia move, a stream flows between the reticular lamina and the tectorial membrane, causing the IHCs cilia to move in the same direction as the OHCs cilia (24). External to the stria vascularis in the bone of the cochlear wall, followed by the spiral ligament, which sits against the bone of the cochlear wall (4).

Sound is converted in the auditory nerve into a nerve impulse’s codes by hair cells in the cochlea, which sends information about the voice that reaches the ear within the hearing range to the brain. Furthermore, the cochlea distinguishes sounds based on their spectrum, thus different frequencies activate distinct populations of outer hair cells (19). The moves of the basilar membrane are converted into a neural

code by inner hair cells in the auditory nerve's fibers. The mature human AN is 22 to 26 mm long and contains around 30,000 fibers (24). Because men's skulls are larger than women's, it is slightly longer in men than in women (24).

Vestibular End Organs

The vestibular labyrinth includes three semicircular canals, each with slightly different diameter: the lateral canal measures roughly 2.3 mm, the posterior canal measures 3.1 mm, and the anterior canal measures 3.2 mm; the otolith organs: sacculus, and utriculus which contain sensory epithelium in semicircular canals; vestibular nucleus; vestibulocerebellum; as well as the vestibular nerve (1). A common bone capsule encloses the utriculus and sacculus, the vestibulum, whereas each semicircular canal is wrapped in its bony shell (1). The alignment of all canals varies from person to person. The canals' inner diameter is between 0.2 and 0.3 mm (29). The bones of the semicircular canals are positioned at 45° (see figure 2.2.) to the planes of the body (coronal, transverse, and sagittal) (1).

The vestibular system maintains visual acuity while moving the head, improves balance control, and recognizes self-motion and gravity orientation (30).

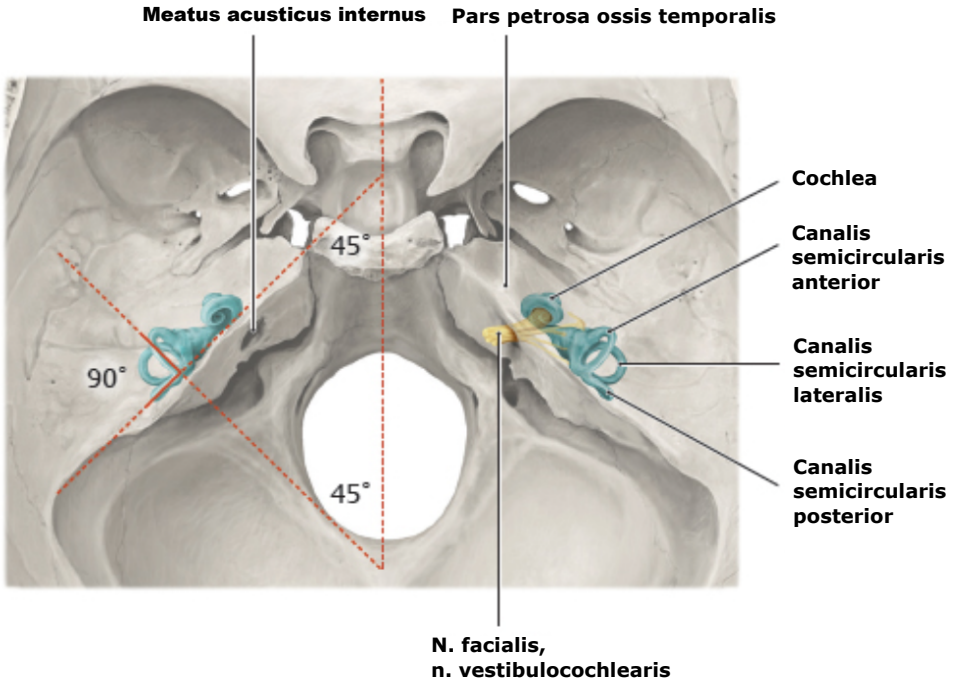

Figure 2.2. The petrous part of the temporal bone from above. The apex of the cochlea is directed anteriorly and laterally. The bone semicircular canals are oriented at 45° to the planes of the body (coronal, transverse, and sagittal). The image has been adapted from Schuenke et al. (1).

2.1.4. Ear: Blood Supply

The vessels are connected by anastomoses and reach the middle ear. All of the vessels that serve blood to the tympanic cavity emerge from the external Carotid A. (1). The vestibular-cochlear A., which supplies the cochlea, is formed when the labyrinthine A. branches farther into the IAM (23). It starts in the anterior inferior cerebellar A. and runs via the IAM, where it branches off into the anterior vestibular A., which supplies the vestibular apparatus. The distance from the horizontal segment of the internal Carotid A., which approaches the cochlea (see figure 2.3.), to the cochlea's basal turn averaged 2.83 mm, with a range from 1.14 to 5.52 mm (31).

Figure 2.3. A histologic slice of the temporal bone at the tensor tympani muscle's level (curved arrow) depicts the petrous carotid's link of the cochlea (double-headed arrow) and the internal auditory canal (short black arrow). The image has been received from Leonetti et al. (31).

2.1.5. Auditory Neuroanatomy

The ectoderm, which separates into the neural lamina in the third week of pregnancy, arises in the whole nervous system. The neuron-to-neuron synaptic connection is one of the most characteristic parts of the nervous system since it is based on the structure of neurons, where dendrites receive information and axons transmit it outside (32). The encephalon, medulla spinalis, and cranial nerves are known as the central nervous system (CNS) (24). The AN connects the cochlea to the brainstem.

The AN axon starts in the spiral ligament and primary afferents of the spiral ganglion that links to the OHCs pass through the Corti tunnel before continuing to the habenula perforata, where they meet up with the fibers from the IHCs (23). The habenula perforata is a bony spiral lamina structure with tiny openings through the primary afferents. The AN's ganglion cells merge in Rosenthal's canal, which is a larger area. (24). The AN travels to the brainstem via a tiny channel in the IAM. Through their axons, the bipolar neurons send impulses to the cochlear nucleus anterior and posterior, which are combined to create the cochlear nucleus (1). The auditory pathway's second neuron receives inputs from these nuclei. Second-order neurons go to the superior olivary nucleus on the other side of the brainstem, where all of the fibers synapses while a few second-order fibers are on the same side (33). The auditory route ascends from the superior olivary nucleus via the lateral lemniscus (34). The nucleus of the lateral lemniscus synapses some of the fibers, but many others bypass it and enter the inferior colliculus, where nearly all of the auditory fibers make a synapse. The route then continues to the medial geniculate nucleus (35). Finally, it follows to the auditory region of the cortex called the primary auditory cortex [Heschl gyrus or Brodmann area (BA) 41-42] (36).

Neuronal networks continue to grow across the brain, becoming more particular as new information is received. The primary auditory cortex (BA 41-42), secondary auditory cortex (BA 41-42), and auditory association cortex (BA 22) are positioned in the temporal lobe among the prefrontal cortex (37). Instead of responding to a wide range of frequencies, most of the sound-responsive neurons react to a narrow range of frequencies by the time the excitation reaches the cerebral cortex (36). Low-frequency tones are often found anteriorly, while high-frequency tones are found posteriorly (38).

2.2. Maturation

According to observations of the human fetus and neonatal ear, the peripheral auditory system is anatomically and functionally mature-like at birth: no substantial growth or change in shape is observed after birth (39). Infants are active listeners, having a robust inner ear and brainstem pathway but a comparatively immature cortex.

They are especially prone to listening to human speech sounds (40). The auditory cortex continues to develop many years after birth.

2.2.1. The Auditory System's Embryonic Development

The structure of the human ear canal continues to develop until the age of seven; in newborns, the canal is shorter and straighter than in grownups (41). The ear canal length increases in the first 24 months of life (42). The pinna grows even in elder individuals. The Eustachian tube shape is normally fully defined at birth, on the other hand, it is more horizontal at birth and in early childhood than it is in maturity (43,44) and it is shorter (21 mm) in a normal 3-month-old than it is in a normal adult (37 mm) (45).

The cochlea, like other peripheral auditory structures, grows rapidly during pregnancy. Surprisingly, the cochlea has grown quite well by the beginning of the third semester, but it is not complete (24). During 4 weeks of development, one of the earliest sensory placodes to arise is the otic placodes, and they help to shape the inner ear structures that control hearing and balance (46). The OC arises as a separate entity between embryonic days (E)11–13, between E13 and maturity, having a narrow and L-shaped cochlear duct that straightens from base to apex before coiling to 1.75 turns. At the same time, cochlear ganglion differentiation begins at the cochlear base in E11–13 and progresses to the apex in E16 (47,48). The establishment of the coiling and elongation of the cochlear duct, as well as the cochlear ganglion, are closely linked in late development (E13 to maturity). These mechanisms also cause the embryonic mesenchyme to differentiate, which assists in the creation of the surrounding osteological structures (49). Between 17 and 19 weeks of gestation (WG), other indications of labyrinth size, for example, the canal and cochlea radius have ceased developing and are became the same size and form as adults. Bone ossification of the surrounding cartilage circles the whole membrane labyrinth during the following two weeks (50).

Both ontogenetically and phylogenetically, the vestibular system is older than the auditory system (40). Around 10 WG, the inner ear's morphological development is complete, with structures such as the endolymphatic duct and SSC (in chronological order, anterior, posterior, horizontal) fully established. Between 16 and 23 WG, the

capsular cartilage enclosing the membrane labyrinth ossifies, forming the actual bony labyrinth (51). The apical part of the cochlea is where maturational changes are most noticeable (52). Like a shred of interesting evidence, robust high-frequency otoacoustic emission responses among newborns have been found while low-frequency responses continue to develop during the early postnatal period and do not appear to be fully developed (i.e., reaching adult-like values) until the age of 6 to 8 years (8).

Synaptogenesis (synapse development) on the outer and inner hair cells is mostly predetermined before birth. After birth, the auditory nerve's synaptic connections should continue to improve (24). The myelination of the auditory nerve, on the other hand, appears to mature throughout the first few months of life. This is based on the discovery of small differences in auditory brainstem response (ABR) latencies for waves I and II in newborns before the age of five months. (53,54).

Maturational changes in the brainstem start with an increase in the size of the pons and midbrain (24). Midbrain development appears to have reached adult levels by the age of six (55). A general increase in the size of the cerebrum occurs after birth; however, complete maturation is frequently not achieved until the age of 20 (24). The cranial vault grows dramatically in size after birth, paralleling the growth of the cerebrum itself, but it virtually ceases expanding after the first decade of life (56). Changes in the thickness, density, and total volume of white matter tracts and cortical grey matter of the brain remain far beyond adolescence (57). The quantity of gray matter in the frontal and parietal lobes reaches a maximum in the frontal and parietal lobes between the ages of 10 and 12. The volumetric peak of gray matter in the temporal lobe does not occur until about the age of 17 (58).

2.2.2. The Temporal Bone’s Embryonic Development

The complicated development and sequence of ossification processes that occur during temporal bone growth (59). Understanding these processes is especially important for understanding how the inner ear, which is a part of the temporal bone, develops. The occipital, parietal, sphenoid, mandible and zygomatic bones articulate with it (60,61). Around 3 WG, the petrous section of the temporal bone begins to produce a membranous labyrinth, which forms the inner ear. In the eighth week of

pregnancy, the squamous component ossifies (60). After all, four ossification centers have united to form a new entity, fast development occurs, and by 16 WG, the bony tympanic ring is nearly entirely grown. The tympanic ring is horizontal at birth, as opposed to angling off the horizontal plane by roughly 55 degrees in adulthood (61,62). Fast ossification of the petrous portion occurs in 20 WG and adult structure of the inner ear in 25 WG (61). As a result, the inner ear does not remodel and is meant to be preserved throughout life, making temporal ossification distinct (60).

In contrast to early-forming components, the squamous, mastoid, and tympanic parts continue to alter their shape and size after birth (63). The mastoid region of the body continues to develop and achieves adult size between the ages of 5 and 10 (61). The styloid process can be developed in a variety of ways. Many ossification centers form at the age of 3–4 years, with the union of various sections occurring during puberty or adolescence (59).

2.3. Growing parts of the body: Head and Height

Children and infants are not miniature humans. In a variety of aspects, their body differs from that of an adult. The brain is usually 25% of its mature size at birth. (64). Changes in body weight follow age-related patterns as well. (65,66).

A newborn's entire height is 50.8 cm on average. During the first year, this height grows by around 25.4 cm. By the fourth year, total height has quadrupled, and by the thirteenth year, it has tripled (20). Growth happens in all three dimensions throughout the postnatal development of the cranium. As the skeleton matures, it expands to the transverse (width), sagittal (anteroposterior depth), and vertical (height), causing a significant difference in the size, form, and proportions of the skull (67). The head is one-fourth of the height at birth, but one-seventh in adulthood (see figure 2.4.). The child's head is thus proportionately bigger than that of an adult (68). The extremities develop faster than the head from the second period of the first year till adolescence (69).

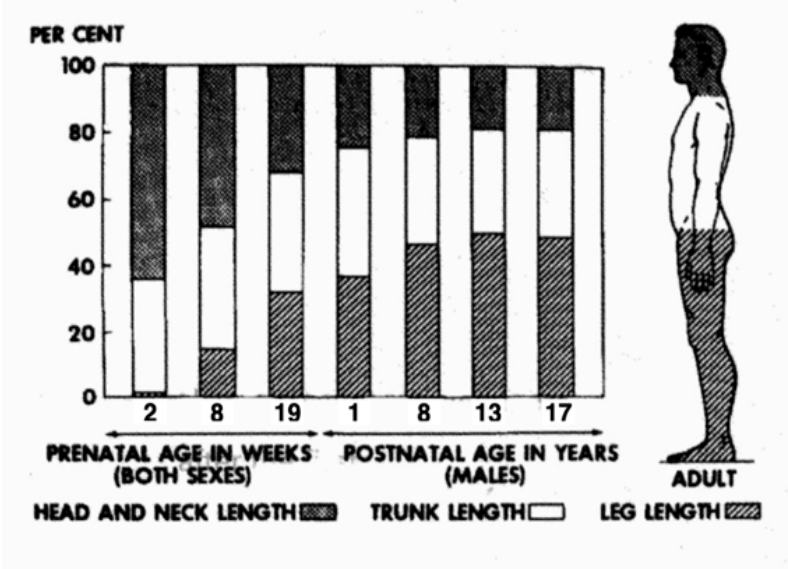

Figure 2.4. The percentage of body segments distribution with prenatal and postnatal developments. The image has been received from Huelke (69).

With a 1:8 face-to-cranium ratio at birth, the face of the skull is smaller than the cranium (compare to the adult ratio of 1:2.5) (69). Because the frontal lobe size of the brain is vast, a newborn's forehead bugles noticeable frontal and parietal prominences concerning the facial profile. The shape of an infant's head is very different from that of an adult. The average circumference of the head at birth is 33.02-35.56 cm. It goes up by 17% in the first three months and 25% at six months. The head circumference only rises by 10.16 cm from the end of the first year to the end of the twentieth (see figure 2.5.)

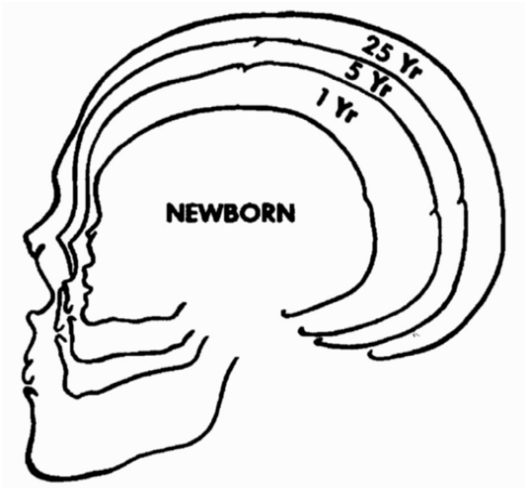

Figure 2.5. Changes in size and form of the skull profiles. The image has been received from Morris (70).

Due to the continuous and fast expansion of the brain as a whole, head circumference grows significantly throughout the first postnatal year. At the age of 7, genetic variables account for more than 70% of the genetic diversity, and at the age of 15, they account for more than 60%. This shows that the eventual head circumference may be predicted genetically from the early stage of life (21). Parts of the brain are exposed to the outer environment and protected by a thin fibrous sheath due to the extensive bone connections. Sutures that fill the spaces between the bones of a baby's skull are more flexible in neonates. These sutures allow the baby's brain to grow in parallel with the skull. About 6-8 weeks after birth, the mastoid suture between the occipital and parietal bones closes. According to several kinds of research, the metopic suture that connects the frontal and parietal bones unite before the life's second (71,72), others claim that the metopic suture starts to unite around the age of two (73).

The proportionality of human development is well-known (10): bigger newborns in terms of height and weight have bigger heads. Furthermore, there are a variety of variables that influence head circumference and height. For example, newborns' height and head circumferences are affected by the mother's height and weight (10,74). Moreover, head circumference is related to gestational age and birth weight (75). The height and head circumference of individuals are assessed in the research including 258 males and 182 females aged 17 to 25 years. The relationship between height and head circumference is statistically significant ($r = 0.443$ for males, $r = 0.302$ for both genders) (17).

2.4. Head Size

There are three types of head structures after defined head length and head height: the chamaecranic (low-skulls), orthocranic (medium-high skulls), and hypsicranic (high skulls) (76). Head length defines as the linear length of the glabella to the ophistocranion points and head height defines as the linear length of the vertex to the pretragus (77). The height-length index is less well-known than the cephalic index, although it has equal anthropological significance. It is a measurement of the height of the skull concerning the length of the skull (78). Individual variance within populations is frequently larger than in the cephalic index, but the environment has a far less impact on the height-length index. As a result, processes like (de-)

brachycephalization have little effect on the height-length index. The mean height-length index in the world is roughly 74. There are the high-skulled and low-skulled tribes on every continent. A flat occipital area is common in the high-skulled groups, whereas a bulged occipital area is common in the low-skulled profiles. The chamaecranic skulls are distinguished by a skull height of less than 70% of the total length (79). The chamaecranics are common among early humans, including the Neanderthals. True chamaecrany is rare today, yet it may be found on all continents. The orthocranic skulls are distinguished by a skull height that is greater than 70% but less than 75% of the skull length (79). The orthocracy is now found throughout the world, particularly in the western half of Europe and considerable sections of South and Central Asia. Skull height reaches at least 75% of the skull length in the hypsicranic skulls. The hypsicrany is now common throughout the South East, Anatolia, America, and middle Europe (78).

Farkas et al. (80) revealed that the developmental level of head length and circumference increased by 5 years, indicating that they were close to maturity. Females achieved full maturity at 10 years old (182.7 mm), while males reached full maturity at 14 years old (189.2 mm). Both genders were approached to the adult head height (113.3 mm in males and 109.8 mm in females) at age of 13 which defined head height differently as the linear length of the vertex to nasion points.

2.4.1. Head Size Measurement History

Aside from height and weight, there are a few more factors to consider, pediatric patients' head circumference (occipitofrontal circumference) is a routine measurement in the study of childrens’ skull growth and brain development, particularly in the first two years of life. It's a quick, easy, and cost-effective screening tape approach that doesn't expose you to radiation (81). Even if head size studies are usually conducted in infants or adolescents, some head circumference charts are also created for adults (82–84).

Head size measurement is important primarily for differential diagnosis (85) as well as for anthropological study (86) The growth of the base of the skull is reflected in the circumference of the head (87). Postmortem studies and CT scans of newborns (88) have shown a substantial positive association between intracranial volume (ICV)

and head circumference, which is consistent with MRI studies of older children (89). For instance, Hshieh et al. (18) investigated 99 older adults (mean = 75.9 ± 4.3 years) who underwent MRI. Statistical Parametric Mapping software and functional MRI were used to assess ICV in three dimensions. The circumferences of the heads were measured with a standardized tape measure (mean = 562.8 ± 21 mm). The measurement was taken outwards from just above the brows to the occipital protuberance. The Software calculates head circumference and ICV are found highly correlated (r=0.73) and by functional MRI found moderately correlated (r=0.69). They found a statistically significant correlation between head circumference and individual height (r=0.46).

3D databases can be collected semi-automatically using CT (90,91) or MRI segmentation, or, utilizing 3D imaging in conjunction with standard head size measurement methods (92,93). For instance, 3D vector analysis is applied to craniofacial CT data, generating 3D cranial surface point clouds. Landmark selection can be done by automatically selecting certain landmarks (such as the nasion, vertex, and eurion) and can be manually defined. Linear distances between landmarks determined in the image generated by the graphic viewer can be measured. With this method, Marcus et al. (94) found that vertex to opisthocranion measurement was 128.94 ± 0.57 mm in the pediatric population (1-60 postnatal week) and nasion to right eurion measurement was 95.97 ± 0.49 mm.

In another study, which measured head by 3D method, a unique photo-optical scanner was used to capture the complete skull of each newborn in a circular pattern in the 6 to 12 months subjects, and the midpoint of the coordinate system is determined as the point where the tragus connecting line intersects. Marcotty et al. (67) selected some reference points such as tragion point, nasion point, occipital point, and measured growth-related parameters: maximum circumference, width, length, and height. For instance, the vertex to the midline of the head was measured as 109.94 ± 0.41 mm.

2.4.2. Head Size Measurement and MRI

Head size visual analysis generally depends on impressions, such as the craniofacial ratio, due to the ability to flexibly zoom an MRI. Repeated clinical tape measurements are unfeasible in clinical practice, highlighting the necessity for an MRI-based approach to determining detailed head size (22).

Rau et al. (22) investigated 85 children (mean age 3.18 ± 2.45 years) to verify an MRI-based method for measuring head circumference. Identify the supraorbital bulge for MRI-based head circumference measurement, then adjust the axial plane in the 3D reformation until the maximum supra-auricular head circumference is attained. The occipital protuberance was used as a reference point. In axial reformat, an ovoid region of interest (ROI) is produced by recognizing the lateral expansion, afterward the anteroposterior expansion on T1-weighted MRI. They found the sensitivity of the MRI-based assessment was 0.97 and accuracy 0.94 when compared with tape measurement and they consider that MRI-based measurement is reliable.

Differently, Vanucci et al. (95) obtained craniometric measures using MRI in 118 individuals, ages ranging from 1 week to 18.7 years to respond to a series of questions on the modern brain's development and its link to people from the recent and distant past. They measured the linear length of the frontal pole to the occipital, vertex to inferior cerebellar margin, etc. using an electronic ruler digital caliper. Mean frontal pole to occipital measurement was found as 154 mm on the mid-sagittal level and they suggested that the head size was bigger than past 40 years ago.

Calderon et al. (96) carried out a study with 49 pediatric participants, between the ages of 5 months and 11 years and MRI phantoms were created using 3D-printed components. Phantom images and head circumference values from 3D objects were obtained analytical then standard head circumference measurements were compared to values acquired from the patients' MRI T1-weighted images. There is no statistically significant difference between the manual and automated assessments ($p = 0.357$). The more error-prone manual head size measurement is supplemented by this automatic application in this study.

2.5. CDL

For years, researchers have studied to assess the length and shape of the human cochlea if there are any changes between individuals and if there are any key characteristics that might help predict a patient's specific CDL (97).

There are significant differences in CDL amongst people (6,9,25,26,98–100). The creation of a preoperative process for estimating the CDL and selecting the proper electrode size is necessary with the introduction of variable length electrodes (101,102). Electroacoustic stimulation, for example, necessitates a lower insertional force during implantation to protect the residual hearing in patients. Because insertional damage is reduced, more hair cells are left alive, resulting in higher postoperative success. (103,104). With a greater understanding of the size of the cochlea and intra-cochlear compartments of the patients, insertional trauma can be reduced (97,105). When measuring the CDL, different imaging technics are used currently. High-resolution multi-detector computed tomography (HRCT) and CBCT are the most common imaging technic (7,106). Ultra-high-resolution multi-detector computed tomography (U-HRCT) is a new kind of computed tomography (14) and microcomputed tomography (micro-CT) (9) and synchrotron radiation phase-contrast imaging (SR-PCI) create ultra-high-resolution images with the highest detail (107). However, micro-CT and SR-PCI technics can only evaluate cadaveric temporal bone specimens (108).

2.5.1. CDL Measurement Methods

Hensen (25) measured CDL 33.5 mm in one ear and 31.0 mm in the other using the direct technique in 1865. The length of the OC is measured by Ulehlova et al. (98) and Wright et al. (109). Both of these direct investigations examine histologic sections to quantify the cochlea's length at the pillar cell union, which is the current standard point for estimating the OC (98,110).

In 1921, Guild (110) set out to develop a consistent procedure for assessing cochlear anatomy using the indirect method. She proposed utilizing histologic cochlea sections 2D graphical reconstructions to determine the estimated lengths of all areas of the OC when sliced in serial portions. On the sections, relevant landmarks were identified and their positions were projected into a 2D plane. In 1953, Schuknecht built

on this idea, aiming to explain the cochlea's three-dimensional shape (111). Hardy (25) was the first to measure the length of the OC using this indirect approach of graphical reconstruction. With an average length of 31.52 mm, it was identical to previous work done utilizing the direct technique. As an indirect method, consistent pictures were obtained from above the plastic-cast cochleae, and the images were utilized to create a 2D reconstruction (6).

Takagi and Sando (112) calculated the length of the cochlea by using computer tools to recreate the 3D structure using coordinates based on histologic sections. The sample cutting angle had a considerable influence on the CDL using the indirect method as compared to the 3D reconstruction methodology (97). The cutting angle effect occurs when the appropriate plane for 2D graphical reconstruction is not used, resulting in a misrepresentation of cochlear dimensions. At the OC, lateral wall (LW), inner wall, and Rosenthal's canal, the final average measurements were 35.58 mm, 40.81 mm, 18.29 mm, and 15.98 mm, respectively. Würfel et al. (27) evaluated cochlear length by employing 3D planar reconstruction and CBCT images. The CDL could only be measured at the LW since the OC could not be seen due to the low resolution of clinical computed tomography (CT) equipment.

Escude et al. (7) establish a technique for calculating approximated lengths of unique cochlea turns that only requires one spiral coefficient. Based on a single surgical measurement, scientists were able to predict where the electrode will be implanted. The 'A' number is the greatest distance between the round window and the opposite LW of the cochlea. Alexiades et al. (5) found the relationship at the OC level, between the A value and the CDL. In a more detailed approach, a 3D reconstruction of the cochlear spiral has been performed on corrosion casts of 108 human cochleae recently, providing a geometric analytical 3D model of the cochlea (4,113).

2.5.2. Cochlear Dimensions

The overall volume of the cochlea is one of the macroscopic properties of the cochlea that is hypothesized to be connected to hearing physiology in animals (114,115), basilar membrane width and length (116), along with the cochlear spiral's number of turns (117), as well as a spiral with a graduated curvature (15) and tightness of coiling (12). For millennia, the form-to-function relationship has been an important question in biology (10). A decrease in thresholds for low and high-frequency

sensitivity has been proposed to relate to the physiology of hearing in apes', with an increase in cochlear cavity capacity relative to body mass (118). As a result, the cochlea of primates is bigger concerning their body mass than that of their close relatives, such as rodents (114). Basilar membranes in mammals that are susceptible to high-frequency sound waves are the thickest and stiffest (119,120). The distance between the primer and secondary bony spiral lamina (the so-called 'basilar gap' of Fleischer) (121) and the 'laminar gap' of Geisler and Luo (122) can be used to measure the width of the basilar membrane is related to the membrane's rigidity.

Perhaps the most evident difference in cochlear anatomy between species is the number of revolutions the spiral completes (see figure 2.6.). In a few Mesozoic species, the cochlea coils from around a single turn to over four turns in caviomorph rodents like guinea pigs in therian mammals (123).

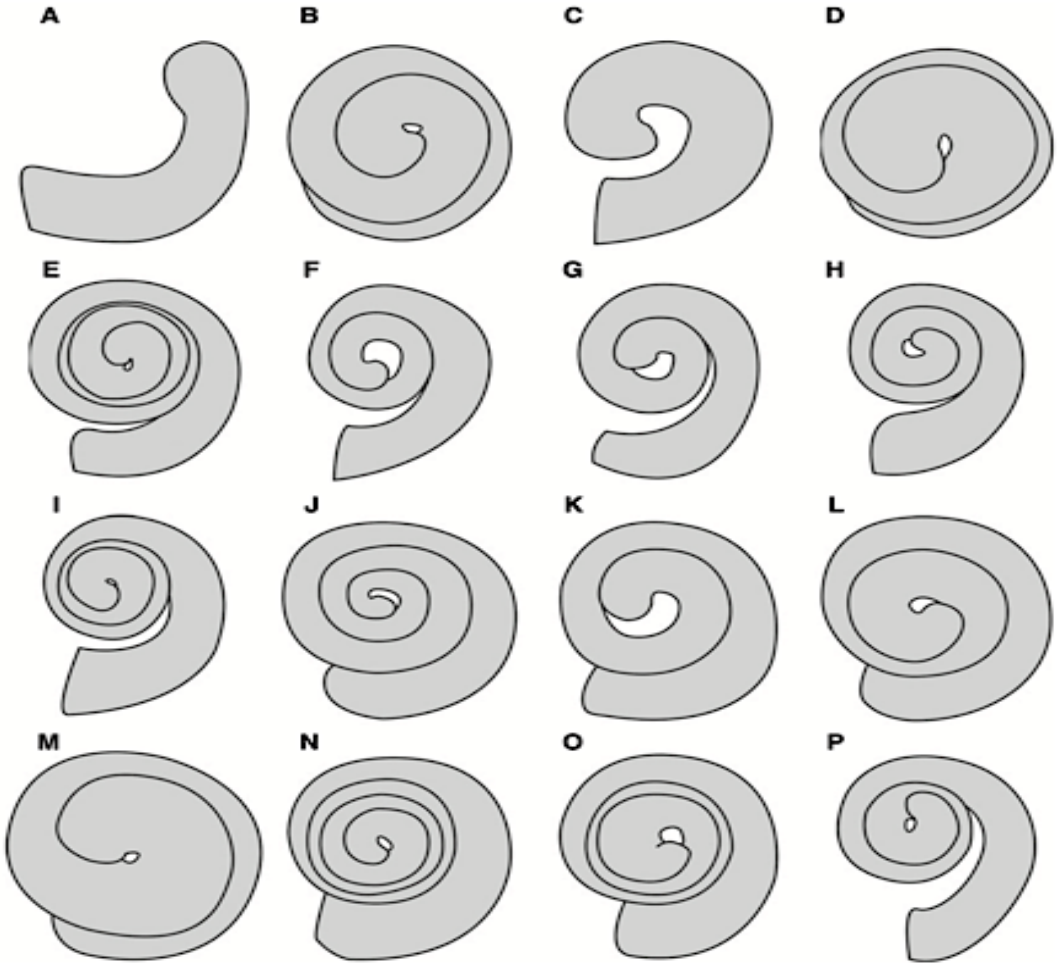

Figure 2.6. Right cochlear line drawings for a variety of animals. (A) Platypus (Ornithorhynchus anatinus); (B) opossum (Didelphis virginiana); (C) Mesozoic eutherian (Kulbeckia kulbecke); (D) elephant shrew (Macroscelides proboscideus); (E) pig (Sus scrofa); (F) humpback whale (Megaptera novaeangliae); (G) bottlenose dolphin (Tursiops truncatus); (H) horse (Equus caballus); (I) cat (Felis catus); (J) greater horseshoe bat (Rhinolophus ferrumequinum); (K) flying fox (Pteropus lylei); (L) cottontail rabbit (Sylvilagus floridanus); (M) house mouse (Mus musculus); (N) guinea pig (Cavia porcellus); (O) tree shrew (Tupaia glis); (P) human (Homo sapiens). The image has been received from Ekdale et. al. (12).

The range of audible frequencies is correlated with the cochlea's total number of turns especially when that figure is multiplied by the cochlear canal's absolute length (15,117). The region of low-frequency sensitivity would be expanded if the cochlear length increased (12).

Another form of function relationship that has been proposed is the distance between successive cochlear turns. After analyzing the cochleae of extinct and present whales, Fleischer (121) found that in toothed whales sensitive to high frequencies, the space between the cochlea’s first and second turns was substantially bigger than in

baleen whales. Cochlear morphological differences that go beyond the number of turns are likely to affect the function of the inner ear's auditory organs (12).

2.5.3. Effects of Cochlear Dimensions

Auditory outcomes such as audibility in lower or higher frequencies may be affected by the cochlear structures (117). Because the overall dimensions of the cochlea are linked to the range of audible frequencies for species, the cochlea may be used to predict hearing capacity (124). The basilar membrane length in terrestrial animals is inversely related to the cochlea's low and high-frequency limitations (117,120,125). Shorter basilar membrane (BM) lengths are related to an increase in high-frequency sensitivity and a decrease in low-frequency sensitivity, respectively. Terrestrial animals with short BM lengths have great high-frequency hearing, whereas those with long BM lengths have excellent low-frequency hearing (120).

Cochlear metrics are rarely measured for each patient, nevertheless, information on the shape of the cochlea to be implanted should always be included before surgery (113). Information on the cochlear metrics allows for the appropriate cochlear coverage to be implanted (6,126,127) and personalized CI maps after surgery (113). In contrast, an accurate representation is required for both clinical estimates of individual frequency maps and preoperative assessment of CI electrode array position and related cochlear coverage. A temporal bone CT scan is routinely used to establish the anatomical status. Due to the limited resolution of CT, the LW is one of the few cochlear structures that can be identified (13).

Cochlear implants employ the tonotopic maps of the cochlea to convey frequency information. Low acoustic frequencies are delivered on the more basal electrodes and so have a lower pitch to a CI user than high acoustic frequencies. The electrode arrays aren't meant to reach the cochlea's most apical regions, which correlate to lower frequencies (13). As a result, the frequencies provided by an electrode array on a cochlear implant, and the frequencies represented at the corresponding place in a normal hearing cochlea may be caused a mismatch. Because prelingual CI users build speech perception primarily through CI, frequency mismatch maybe just a difficulty for postlingual CI users. Deviations from natural frequency locations, on the other hand, may decrease performance, increase the time it takes for a CI user to achieve

asymptote performance, and low quality of the sound (13,102,128). On the other hand, the difference between the basal and apical turns in diameter of the cochlea appears to be associated with low-frequency sensitivity (129).

When it comes to deeper insertion of the electrode array, the first theory (13,130) argues that apical stimulation reduces mismatch, while others (131,132) argue that it confuses the apical frequency range, produces damage, and decreases stimulation at the basal turn (14). According to Buchman et al. (130), users of a 31 mm electrode array get asymptotic performance quicker than 24-mm electrode array users. Roy et al. (133) investigated whether the insertion angle affects low-frequency information discrimination in musical sound quality. Deeper insertion angles allowed CI users to improve low-frequency perception and better sound quality that were more comparable to normal hearing controls. According to Kuthubutheen et al. (11), CI users with the 28 mm electrode array and the 31.5 mm electrode array were examined with hearing in noise test (HINT) phrase evaluations and consonant-nucleus-consonant (CNC) word scores 6 months after surgery and those larger cochlear diameters were linked to better speech performance (117).

Having cochlear dimensions information can result in less damage during surgery and better frequency matching. When looking at the effect of angular insertion depth on speech perception, O'Connell et. al. (134,135) found that for every 10 degrees of angular insertion depth increase, the CNC word score increased by 0.6%. Buchner et al. (136) found that the users with the 31.5 mm electrode array had a substantially higher speech perception score than users with the 24 mm electrode array in 13 subjects. Studies found a 40% significant correlation between angular insertion depth and speech perception in the first year, whereas studies that looked at speech perception in the second year or later found 14% (14). In terms of early and late outcomes, the brain may adjust to a variety of changes within a year. Plasticity is a significant consideration.

2.6. Spiral Shape of The Cochlea

Modern animals' coiled cochlea is an important evolutionary innovation. The nautilus shell is a renowned emblem of hearing due to its resemblance to the cochlea (10). The outer framework (otic capsule), is made of hard bone and forms a spiral cone

shaped like a snail that protects the membrane cochlea (24). However, the reason for the inner ear's spiral shape remains confusing (4). Different theories have been put forward regarding the causes of the spiral shape.

2.6.1. Shell Theory

Physical and biological variables have a formative influence on an organism's appearance, which may be revealed through the mathematical investigation of its shape (10). The connection between auditory nerve fibers' typical frequency and the cochlear site they innervate is logarithmic (125,137,138). The nautilus shell has an outstanding similarity with the logarithmic Fibonacci spiral (139). The nautilus shell, on the other hand, extends from the inside out, adding chambers as it grows, with the outside (larger) chambers resulting from the earlier chambers and nutritional richness. The cochlea is distinguished from the otocyst by the fact that it develops in the opposite direction (51). As a result, the origins and known constraints of the cochlea and nautilus morphologies point to quite different systems (140).

2.6.2. Whispering Gallery Theory

The cochlear shape has inspired several practical hearing solutions in the past. The inner ear is thought to serve as a whispering gallery, concentrating low-frequency tones to the cochlea’s apex, and hence takes an acoustic role due to its structure (15,141–143). The cochlea can distinguish between different frequencies because they peak at distinct locations along the cochlear duct. This peak location has been proven to be unaffected by the spiral structure of the cochlea; in principle, a straight, unrolled cochlea should work similarly. As the wave progresses, more energy accumulates towards the outside edge of the spirals, rather than being equally spread across them (15). Low frequencies have the most significant impact since they enter the spiral the furthest. This concentration of sound intensity leads to greater sensitivity because the cells that perceive vibrations respond very effectively to pressure variations between the inner and outer borders. The sound propagation is likened to the "whispering gallery model" designed for St. Paul's Cathedral in London, where even low sounds may travel long distances without losing energy, skipping down a cylindrical wall. On the other hand, the mild spiral offers vibrations traveling down the cochlea a unique

twist: the ever-tighter twists guarantee that sound rays focus gradually closer to the wall. The cochlea's spiral design improves its capacity to detect low-frequency sounds (15). Conversely, the cochlear shape is very diverse from person to person. This heterogeneity is incompatible with the acoustic whispering gallery's function (4).

2.6.3. Efficient Packing Theory

Efficient packing theory is the most discussed theory recently. The inner ear's form is the result of space constraints within the petrous bone. Local factors have a substantial influence on morphogenesis (144). While looking at phylogeny and mammals, Luo et al. (48) suggest that Dryolestes, a Late Jurassic animal, has evolved bone features of therian-like innervation in comparison to present therians. Because it has a less developed cochlear canal than modern therians' coiled cochlea, innervation resembling that of a therian evolved before the completely coiled cochlea. Dryolestes' cochlear innervation is the preliminary condition for the curve to coil transition in mammalian phylogeny.

The development of the cochlea is controlled by a network of genes (145,146). Genes are involved in the epithelia-mesenchymal interaction, in which the sensory epithelium and neural tissues help adjacent mesenchyme precursors morphogenesis to bone development via chondrogenesis and osteogenesis (48). As a result, there are a variety of cochlear specializations in placental animals that relate to hearing range in adaptation to different surroundings, all of which are based on the same basic structure. Although there is no significant correlation between the length and number of turns of the cochlea, it has been proposed that cochlea coiling is a mammalian adaptation to overcome a packing difficulty caused by the basilar membrane's lengthy elongation (106,116).

The relationship between intraspecific morphological variations and physiological differences is uncertain. The length of the cochlear canal, for example, was shown to be related to body mass (129), however, it's unclear whether larger people are exposed to a wider or narrower frequency range than smaller persons of the same species. The number of turns does not have a significant relationship with body mass in most species, and the degree of coiling does not vary considerably (123).

Pietsch et al. (4) grouped individual cochlea according to cochlear profiles. Human cochlea with smaller bases was more wrapped, which might explain interindividual wrapping variation as a result of space restrictions during ontogenesis. Space limitations within the petrous bone are the most likely cause of the spiral form and substantial interindividual variability. Because of the numerous spatial restrictions, the form has multiple anatomical origins, such as the location of brain structures influencing the cochlear spaces. Genes (48) and individual spatial constraints during ontogenesis, co-determine cochlear shape.

3. PARTICIPANTS AND METHODS

This retrospective study was conducted within the scope of the Master of Science program in Audiology (Department of Audiology, Graduate School of Health Sciences, Hacettepe University, Ankara, Turkey) in collaboration with the Auditory Neuroscience Laboratory (Department of Experimental Otology, Hannover Medical School, Hannover, Germany). Ethical approval was obtained from the Hannover Medical University (Protocol no: 18972013). The participants consisted of a group of patients who have been followed up at the Medical University of Hannover for CI candidacy. Hence, their existing preoperative CBCT and MRI findings were screened retrospectively to select the patients to be recruited in the present study sample.

3.1. Participants

The study participants were 112 adults, assessed previously with CBCT and MRI for CI candidature. The group consisted of 69 females (%61.61) and 43 males (%38.39). Their ages ranged from 22 to 96 years. The details of the demographic characteristics of the subjects were given in Table 3.1.

Between July 2010 and June 2021, eligible participants had their temporal bones anatomically evaluated as part of a regular clinical visit for various diagnoses of hearing loss and/or tinnitus. However, detailed auditory evaluation results of the subjects were not available in the database. 112 participants were selected based on the following criteria. Potential subjects were ruled out, if they 1) had temporal bone and inner ear disorders, either acquired or congenital 2) did not have detectable cochlea in both temporal bones 3) did not have a good resolution MRI of the head 4) less than 18-year-old and 5) movement artifact or incomplete visualization of the cranium. MR images of patients were obtained from Visage 7 imaging software, which allows virtual access to all data.

Table 3.1. Demographic information of participants.

		Mean	Sd	Min	Max
Age (years)	**F (n=69)**	61.59	19.78	22	94
	M (n=43)	69.53	14.21	26	96
	Total (n=112)	64.6	18.03	22	96

F: female, M: male, Sd: Standard Deviation, Min: Minimum, Max: Maximum).

All participants were postlingually and bilaterally deafened. CDLs from 29 unilateral CI users were measured specifically for the ear to be implanted (right CDLs n= 102, left CDLs n= 91). For the selection of the study ear in bilateral CI users (n= 83), a statistical analysis was performed to investigate CDL differences between the right/left ears. Within-subjects comparisons did not show any statistically significant differences between the ears ($p>0.05$). Hence, CDL data was obtained from the left ear for participants with bilateral implantation.

3.2. Materials and Methods

The present thesis was based on a retrospective study. Clinical information, such as the participants' gender, age, height, and CDL, were obtained from the database of Hannover Medical University.

3.2.1. CDL Measurement

The cochlear duct length was measured as described previously by Würfel et al. (27). A fixed Xoran MiniCAT (Ann Arbor, Michigan) with a 536 x 536 matrix detector resulting in 0.3 mm^3 isotropic voxels (125 kVp, 7 mA) and a mobile Xoran xCAT (Ann Arbor, Michigan) with a 536x536 matrix detector resulting in 0.3 mm^3 isotropic voxels (125 kVp, 7 mA) was used to collect temporal bone CBCT data (120 kVp, 7 mA). OsiriX MD (Pixmeo, Los Angeles, California) based on DICOM data using 3D curved MPR.

The round window's distal bony rim acts as the origin. The curve was generated in 3D along the bony cochlea's outer border in the projection of the bony spiral lamina. The endpoint was specified as helicotrema. The interface included four windows, one for each segment and one for the uncoiled spiral.

When measuring the cochlea, in the interface’s first window, the beginning point was defined as a round window in the basal turn. The continuous basal turn and the round window were shown in the interface’s second window. The interface’s third window displayed the modiolus section which was positioned orthogonally to it. The interface’s first window was placed within and parallel to the second window's basal turn. The manually measured spiral set point along the bony outside border of the cochlea was determined. The endpoint was defined as the helicotrema.

CDL was measured in both temporal bones of 84 participants, only the right ear of 21 subjects, and only the left ear of 7 subjects (a total of 69 females and 43 males), for a total of 196 measurements. CDL measurements were obtained retrospectively.

3.2.2 Head Size Measurement

In the present study, all reference points chosen in MR images could be identified. The imaging was performed for clinical reasons, and the settings were chosen to provide the cochlea with the best visibility possible. T1 (transverse relaxation time 1)-weighted and T2 (transverse relaxation time 2)-weighted MRI images were used. T2 scans were first employed, which had a longer repetition time (TR) and time to echo (TE) of roughly 4000 and 90 msec, respectively. As a result of this, cerebrospinal fluid (CSF) brighter on T2-weighted imaging subsequently made it easy to work on cochlear structures. That is, an axial image from MRI (also known as a transverse or horizontal plane) which was an image parallel to the ground, separates the superior from the inferior which elucidates both of the cochleae were applied. In addition, an external view of the head T1-weighted imaging without multiplanar reconstruction (MPR) or reformatting that of the original stack which was extracted from Visage 7 imaging software MRI data was applied to all patients.

MR images of patients were extracted as DICOM images. DICOM images processing was performed with 3D SLICER version 4.11.20210226 for Windows 10 image computing open-source and image computing platform software. Axial T2-MR image and external view of the head T1-MR image were processed in 3D-by-3D Slicer.

The first subject was selected randomly to transform MR images into 3D and to determine reference points for that. Bringing the MR images to the aligned plane required expertise and to do this a special amount of time was spent. Namely, if the MR images were rotated to one direction or if they were tilted, then, they were aligned via transform option that enabled images to be rotated in 3D until 3D coordinates (while moving forward from vertex to the midline and on the left and right side of the same structures) became identical. In this alignment process, the heads were visualized at the transverse plane. This transverse plane was determined when progressing from the vertex of the head down ventrally from the longitudinal axis, to the midline, the

section plane in which were first encountered superior semicircular canal, visible as a small less dense spots of one or only a few voxels, was chosen as a reference plane in the sagittal-inferior direction. This was optimal due to the small size of these orientation spots.

An example of the alignment process, is the end of the basal turns of both sides, which is described as a cochlear lateral wall (visible as a small less dense spots of one or only a few voxels), at the transverse plane (see figure 3.1.), were rotated on the x,y and z coordinates until they were aligned on the same position. Simply, it was decided by looking at the y and z coordinates for both sides were equal but these points were located in different x coordinates: right and left. All participants' MRIs were rotated in this manner.

At the same reference plane, the points encountered with the one or few voxels of the superior semicircular canal walls (see figure 3.2.), going from the vertex to the head down ventrally were chosen as well. These points defined the first point of the superior semicircular canal on the transverse plane.

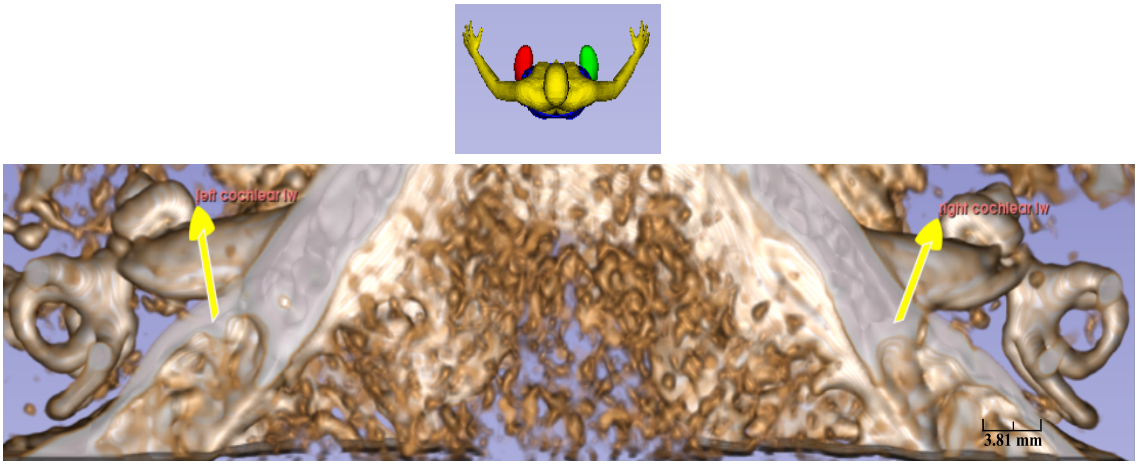

Figure 3.1. Cochlear landmarks in superior view of the head.

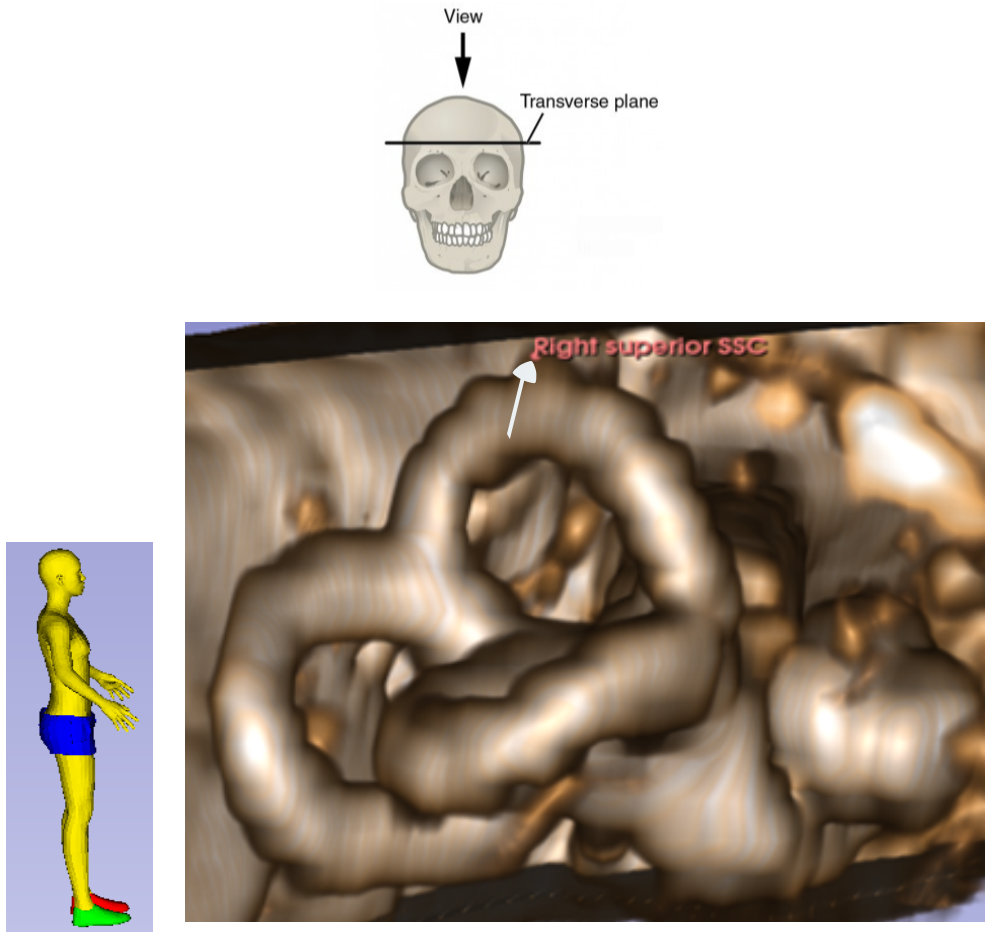

(a)

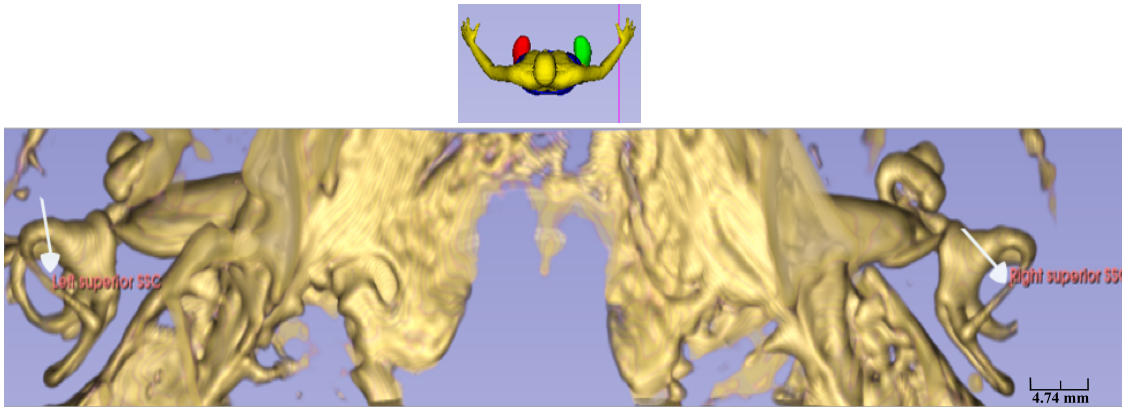

(b)

Figure 3.2. (a): Right superior SSC reference point which first encountered with superior SSC by transverse plane in the lateral view. (b): Both superior SSCs were visible in the superior view of the head.

Basilar A. is defined as first encountered with the image of the entire circle of the basilar A. after going ventrally in the axial image. Before choosing landmarks in this section, images were divided into equal-length-squares, then the middle of the arteries was chosen. Herewith, in the same section middle of the left and right-side Carotid A. was determined as reference points (see figure 3.3.) as well as both carotid arteries' y and z coordinates were determined on the same coordinates. So, those inner points were equidistant from the face and vertex.

On the external view of the head, T1-weighted imaging is converted into 3D and divided into squares of the equal-length-squares via the transform option in the 3D Slicer to choose reliable reference points of equal length to a landmark. Bilateral reference points were 1.20 cm anterior to the tragus midline, and they were determined as the zygomatic arch's beginning area on the ear side in the literature (147). This point was called pretragus in the present study (see figure 3.4.).

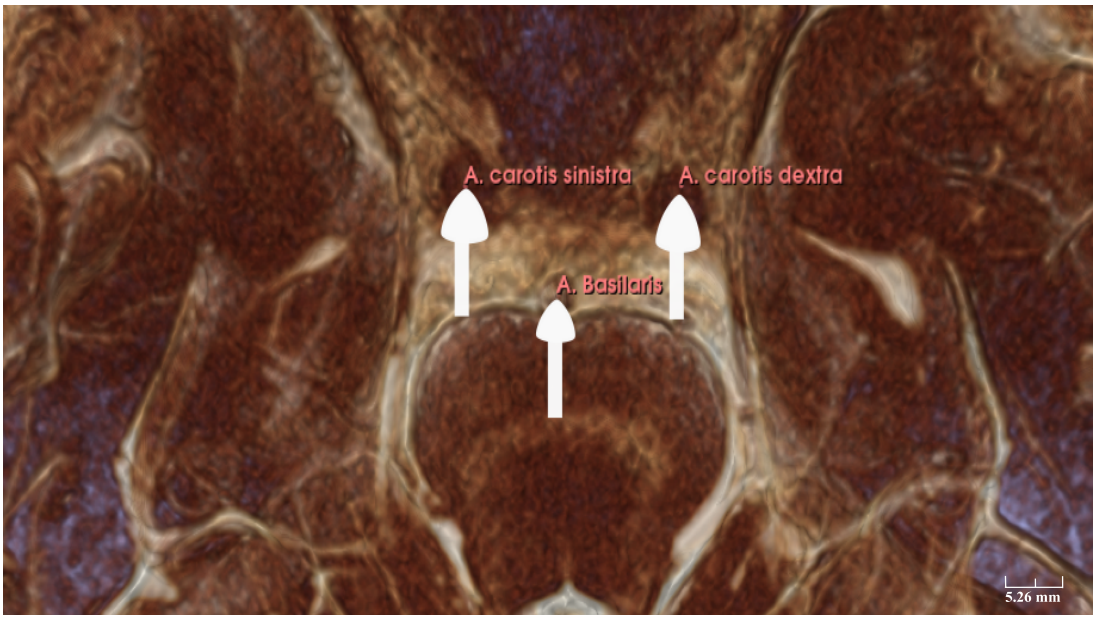

Figure 3.3. Basilar A. and Carotid arteries. Both side of the Carotid arteries were chosen as reference.

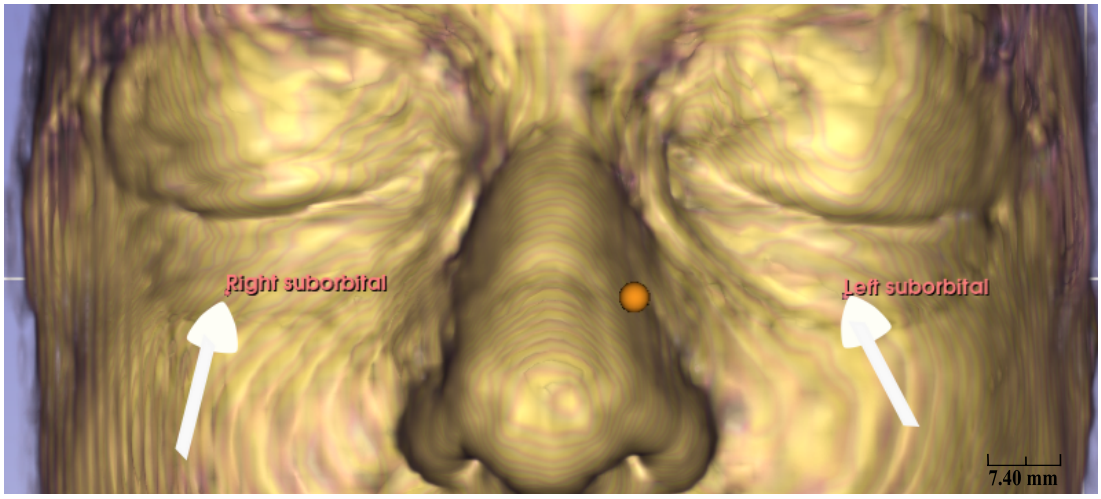

(a)

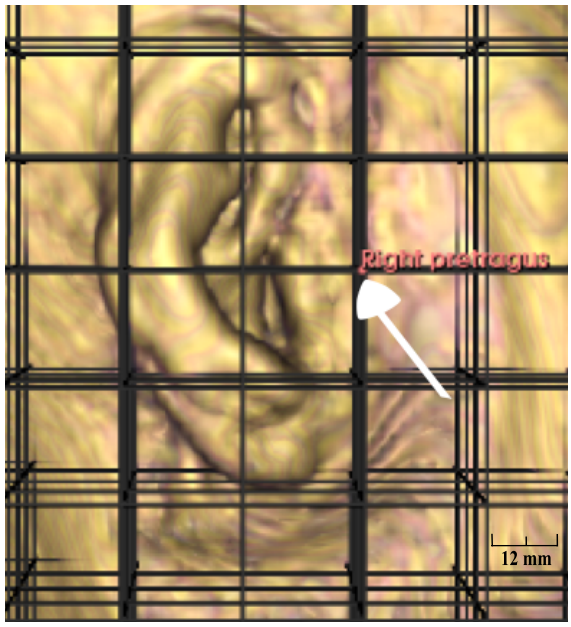

(b)

Figure 3.4. (a): Suborbital left and right. An anterior view of the head indicated the left and right suborbital on the tear trough sulcus. (b): Right pretragus. The lateral view of the head was divided into squares of equal length and the reference points were 1.20 cm anterior to both of the tragus, and they were the zygomatic arch's beginning point on the ear side.

Left and right suborbital (or infraorbital) which is on the tear trough sulcus lower limit of the orbital septum (148) and the end of this line, junction point with palpebromolar groove chosen as reference points (see figure 3.4.). They are located inferior to the middle of the eyes. Another reference point was occipital protuberance (also known as external occipital protuberance or opisthocranion) close to the inion which is the highest point of the squamous section of the occipital bone, and it is

located in the center of the squamous part of the occipital bone. The pretragus, suborbital and occipital points are specified in the horizontal plane, according to the Frankfort horizontal plane, which is widely used. And the last one was the vertex which is located medially on the midscalar region of the top of the head (149) (see figure 3.5.). Vertex and occipital protuberance points had been defined similarly for anthropometry studies (76,77).

After the reference points of the first subject were saved in fcsv format, the MR image of the subsequent subject was opened with the first points chosen. And the first reference points coordinates were changed to 3D until these points' appearances were quite suitable for the new subject's head.

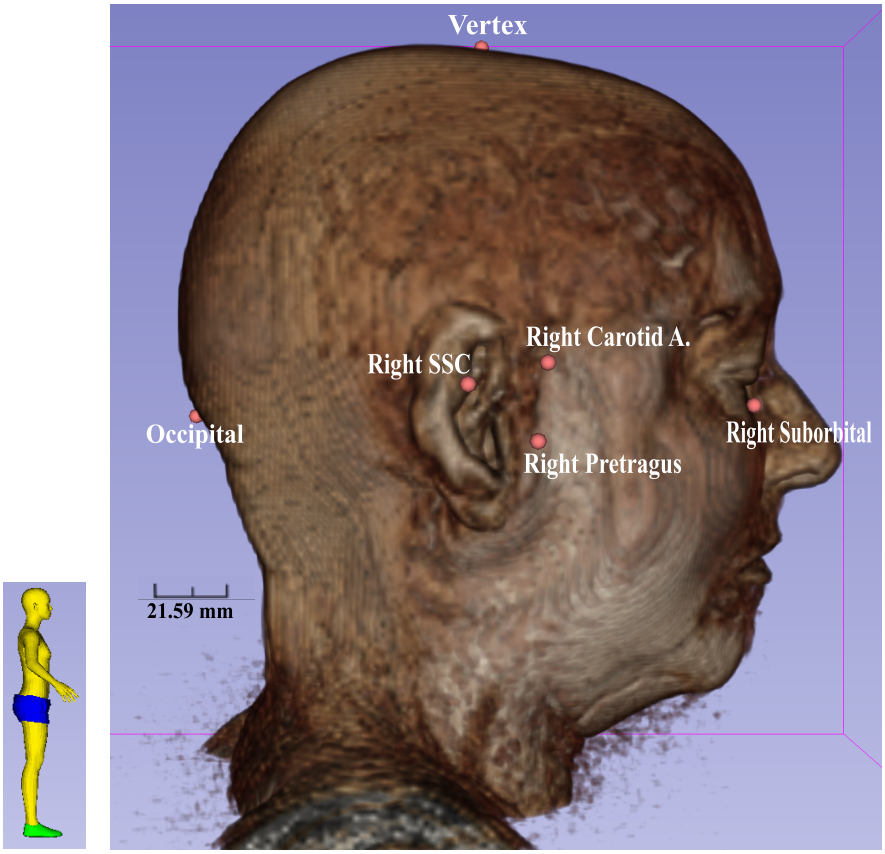

Figure 3.5. The right lateral appearance of all right landmarks. The sagittal placement of all markers could be seen even if the right SSC and right Carotid A. were selected inside the skull rather than on the skull. Occipital protuberance, vertex, right pretragus, right SSC, right Carotid A., and right suborbital markers were visible.

Saving the reference points for all patients in fcsv format, the corresponding files were imported into MATLAB (versionR2018a). The Euclidian distances between all points were computed for each patient and exported in xlsx format for further evaluation.

Linear lengths between two points were chosen to give information about the head size on the sagittal, coronal and transverse planes and selected the most appropriate measures for all planes in which the cochlea is located. Linear distances between certain two points were calculated as previously explained. All of these measures: left and right suborbital to occipital; left to right pretragus; vertex to left and right pretragus, which is called head height in the literature (77); vertex to left and right superior SSC; left superior SSC to right superior SSC; left Carotid A. to left suborbital and right Carotid A. to right suborbital (see figure 3.6.).

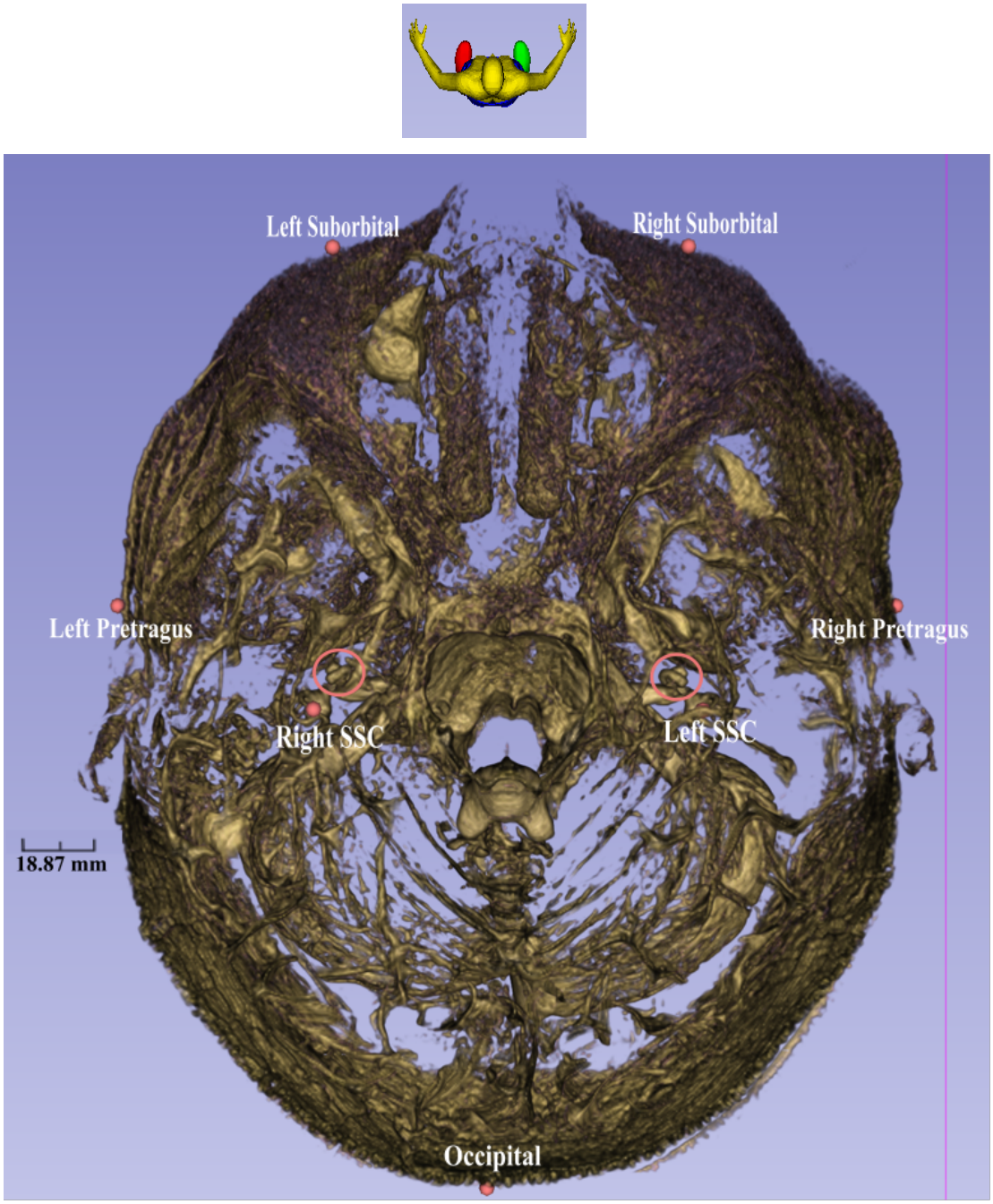

Figure 3.6. The pretragus, suborbital, and SSC landmarks on both sides were visible in a coronal view. Both circles indicated the cochleae on both sides.

3.3. Statistical Analysis

Statistical analysis was performed using Statistical Package for Social Sciences (SPSS) version 26.0 (Chicago, USA). The normality of the data was evaluated with the two-tailed Kolmogorov-Smirnov test. Normality tests were carried out by checking skewness, histogram, and Kolmogorov-Smirnov test. The equality of variances for all variables was assessed by using Levene's test of homogeneity ($p > 0.05$). Parametric tests were used for statistical analysis since the Kolmogorov-Smirnov test confirmed the normal distribution of the CDL, head size, and height data ($p > 0.05$). Bivariate correlations between variables (age, CDL, head size, height) were investigated with the Pearson correlation coefficient (two-tailed test). The independent sample t-test was performed to determine the gender differences. Correlation coefficients were considered very high when $R > 0.80$, high when $R = 0.60$-0.80, medium when $R = 0.40$-0.60, weak when $R = 0.20$-0.40 and very weak when $R < 0.20$. The cut-off level for significance was set to 0.05.

4. RESULTS

CDL Findings

Present CDL findings consisted of 112 ears (mean CDL= 37.04 ± 1.91 mm, range 42.9 to 30.8 mm). The descriptive statists for CDL were shown in Table 4.1. Bivariate correlations based on data from 83 bilateral participants showed very strong positive correlations (r=0.92, p<0.001) for within-subjects right versus left ear CDL comparisons. The mean CDL for males (37.42 ±1.87 mm, range 32.7 to 42.2 mm) was longer than that for females (36.80 ±1.91 mm, range 30.8 to 43.2) (see figure 4.1.). The CDL differences between males and females were not statistically significant [(t (110)= -1.703, p= 0.091]. The age did not show any statistically significant effects on CDL findings (r=- 0.07; p= 0.463).

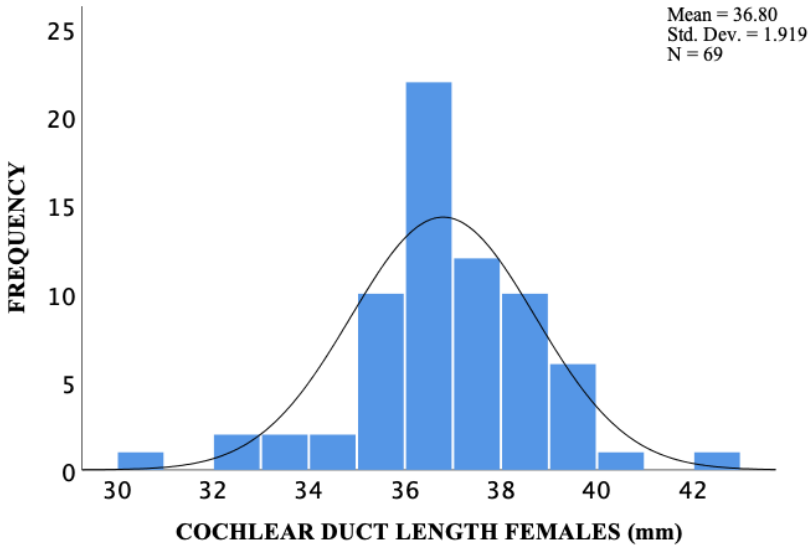

(a)

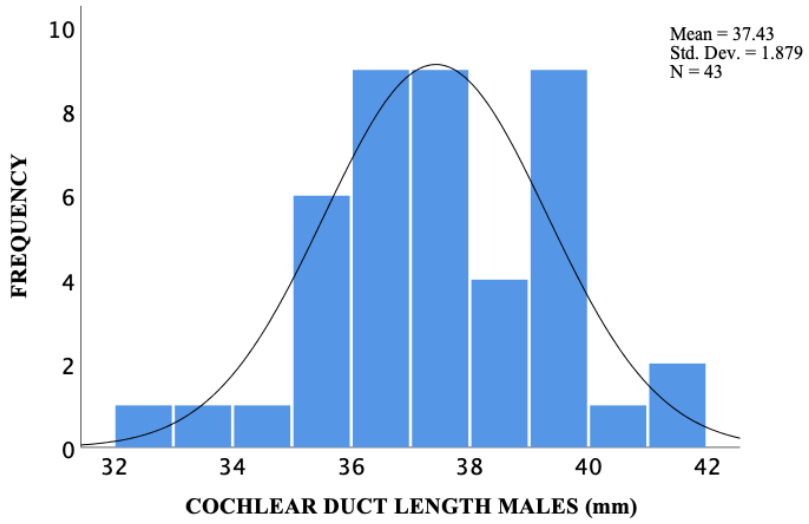

(b)

Figure 4.1. (a): CDL's frequency histogram for females (n=69). **(b):** CDL's frequency histogram for males (n=43).

Table 4.1. Descriptive statistics of CDLs according to the genders (n=112).

		Mean	Sd	Min	Max
CDL (mm)	**F (n=69)**	36.8	1.91	30.8	42.9
	M (n=43)	37.42	1.87	32.8	41.7
	Total (n=112)	37.04	1.91	30.8	42.9

Head Size Findings

The present head size measures consisted of 112 participants. The descriptive statists for head size measures between the landmarks were shown in Table 4.2.

Head size measures based on the different landmarks were significantly correlated with each other. Moreover, the correlations between the left and right-side measures were statistically significant (see Table 4.3.). Figure 4.2. represented statistically significant positive correlations for left versus right suborbital to occipital protuberance measures ($r= 0.99$, $p< 0.001$). The present findings showed larger head size measures for the males than those for the females (see figure 4.3.-4.4.) and the differences were statistically significant ($p< 0.05$) (see Table 4.2.).

Table 4.2. Descriptive statistics of head measures according to the genders (n=112).

	Gender	Mean	SD	Gender Differences
Right - Left Pretragus (mm)	**F**	**149.89**	10.58	t (110) = -3.903 p< 0.001
	M	**157.76**	10.02	
	T	**152.56**	11.01	
Left Suborbital – Occipital (mm)	**F**	**177.32**	9.94	t (73.102) = -4.729 p< 0.001
	M	**188.16**	12.80	
	T	**181.46**	12.27	
Right Suborbital - Occipital (mm)	**F**	**177.10**	10.04	t (74.949) = -4.801 p< 0.001
	M	**187.96**	12.53	
	T	**181.27**	12.22	
Left SSC - Right SSC (mm)	**F**	**77.69**	4.87	t (72.035) = -3.509 p< 0.001
	M	**81.69**	6.40	
	T	**79.13**	5.82	
Vertex - Left Pretragus (mm)	**F**	**148.59**	7.85	t (110) = -4.569 p< 0.001
	M	**155.52**	7.70	
	T	**151.26**	8.46	
Vertex - Right Pretragus (mm)	**F**	**148.40**	8.02	t (96.799) = -4.716 p< 0.001
	M	**155.28**	7.16	
	T	**151.13**	8.37	
Vertex - Left SSC (mm)	**F**	**119.63**	6.86	t (110) = -3.597 p< 0.001
	M	**124.22**	6.06	
	T	**121.42**	6.91	
Vertex - Right SSC (mm)	**F**	**119.36**	6.44	t (110) = -3.808 p< 0.001
	M	**124.07**	6.24	
	T	**121.20**	6.74	
Occipital - Vertex (mm)	**F**	**154.34**	6.36	t (67.983) = -4.570 p< 0.001
	M	**161.55**	9.04	
	T	**157.11**	8.25	
Left Carotid A. - Left Suborbital (mm)	**F**	**74.06**	7.09	t (102.83) = -2.987 p= 0.004
	M	**77.73**	5.78	
	T	**75.42**	6.83	
Right Carotid A. -Right Suborbital (mm)	**F**	**73.80**	6.91	t (103.201) = -3.540 p= 0.001
	M	**77.99**	5.52	
	T	**75.36**	6.71	

The value of mean, standard deviation (SD), and statistical gender difference t-test results were given.
F: female, M: male, T: total, SD: standard deviation, LW: lateral Wall, A.: Artery.

Table 4.3. Head size measures correlations with each other.

	Right-Left Pretragus	Left Suborbit-Occipital	Right Suborbit-Occipital	Left SSC - Right SSC	Vertex - Left Pretragus	Vertex - Right Pretragus	Vertex - Left SSC	Vertex - Right SSC	Left Carotid A. -Left Suborbit	Right Carotid A. -Right Suborbit	Vertex - Occipital
Right - Left Pretragus	**1**										
Left Suborbit - Occipital	**r=.49****	**1**									
Right Suborbit - Occipital	**r=.50****	**r=.99****	**1**								
Left SSC - Right SSC	**r=.47****	**r=.27****	**r=.29****	**1**							
Vertex - Left Pretragus	**r=.37****	**r=.39****	**r=.39****	**r=.23****	**1**						
Vertex – Right Pretragus	**r=.42****	**r=.45****	**r=.45****	**r=.19***	**r=.92****	**1**					
Vertex - Left SSC	**r=.32****	**r=.47****	**r=.47****	**r=.26****	**r=.55****	**r=.56****	**1**				
Vertex - Right SSC	**r=.32****	**r=.48****	**r=.47****	**r=.25****	**r=.59****	**r=.62****	**r=.90****	**1**			
Left Carotid A.- Left Suborbital	**r=.35****	**r=.44****	**r=.40****	**r=.20***	**r=.23****	**r=.25****	**r=.29****	**r=.28****	**1**		
Right Carotid A.- Right Suborbital	**r=.38****	**r=.45****	**r=.43****	**r=.23***	**r=.26****	**r=.29****	**r=.30****	**r=.28****	**r=.95****	**1**	
Vertex - Occipital	**r=.23****	**r=.61****	**r=.60****	**r=.13**	**r=.60****	**r=.61****	**r=.52****	**r=.58****	**r=.28****	**r=.28****	**1**

**: Correlations were statistically significant at the p=0.01 level, *: Correlations were statistically significant at the p=0.05 level. Gray cells demonstrated left versus right side measure's correlation coefficient.

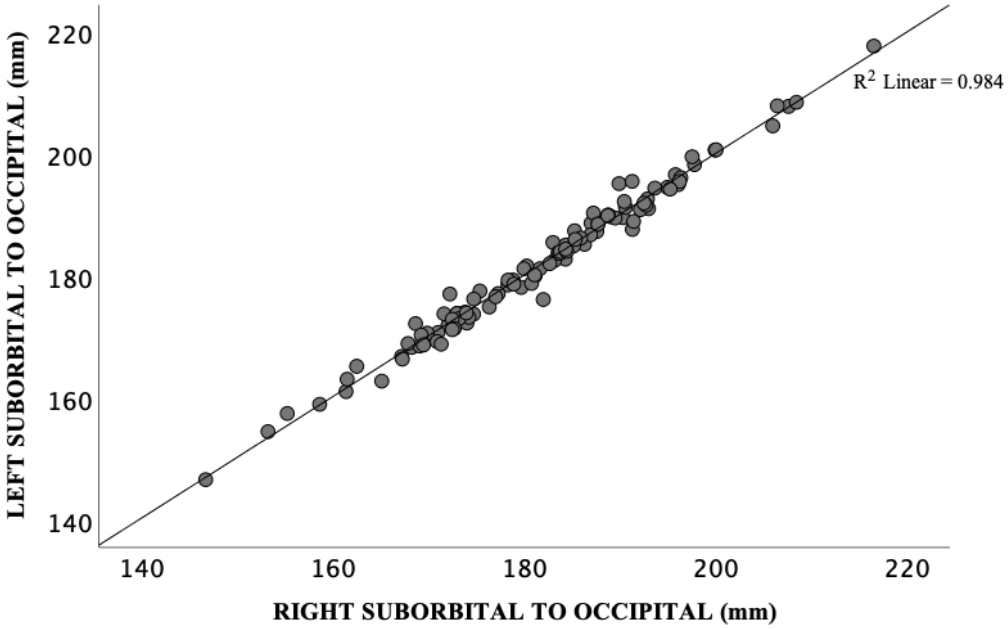

Figure 4.2. The correlations were statistically significant for right versus left side head measures. The figure represented left suborbital to occipital protuberance measures' correlations with right suborbital to occipital protuberance measures (r= 0.99, p< 0.001).

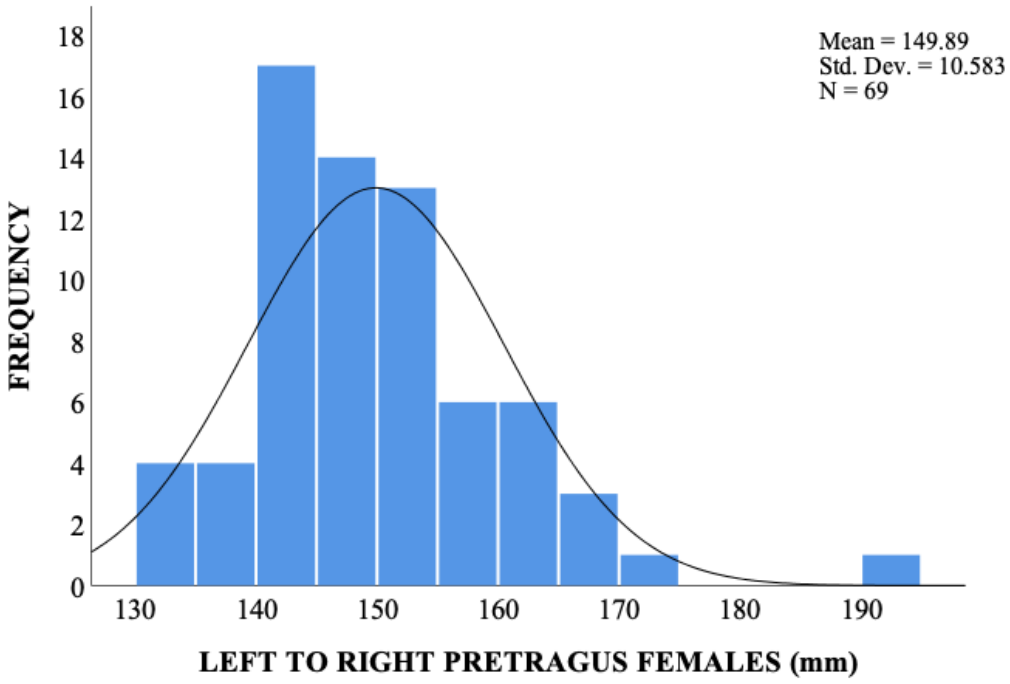

(a)

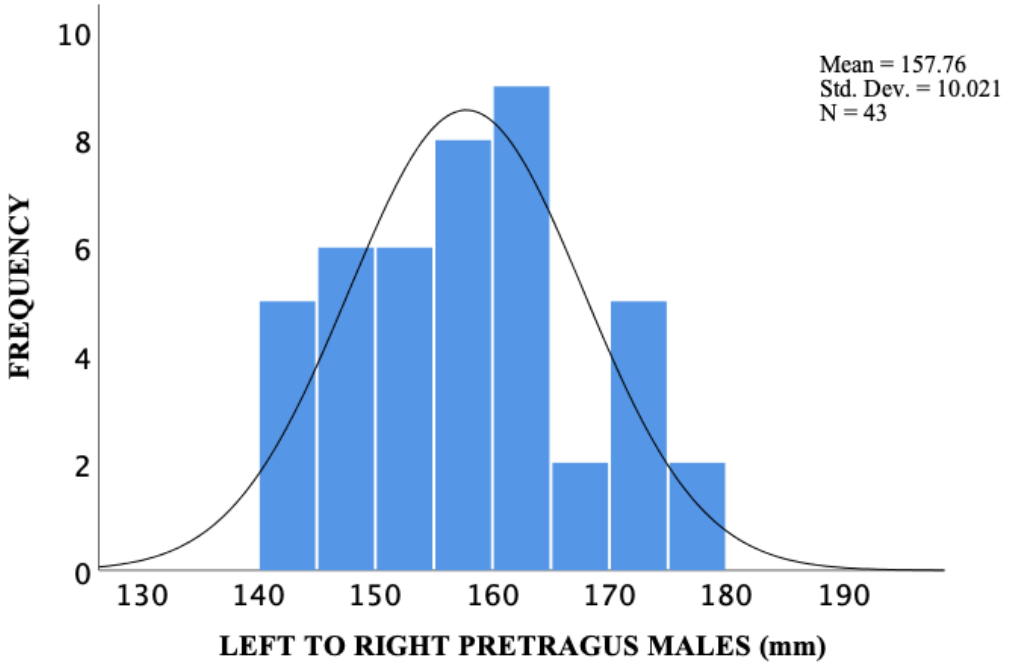

(b)

Figure 4.3. (a): Left to right pretragus measures' frequency histogram for females (n=69). (b): Left to right pretragus measure's frequency histogram for males (n=43).

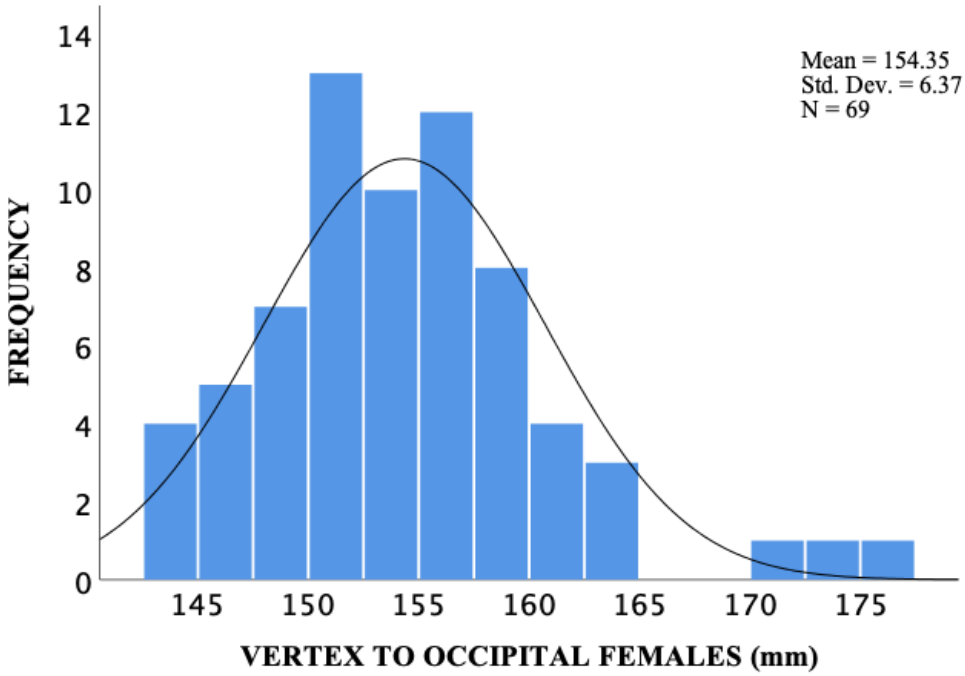

(a)

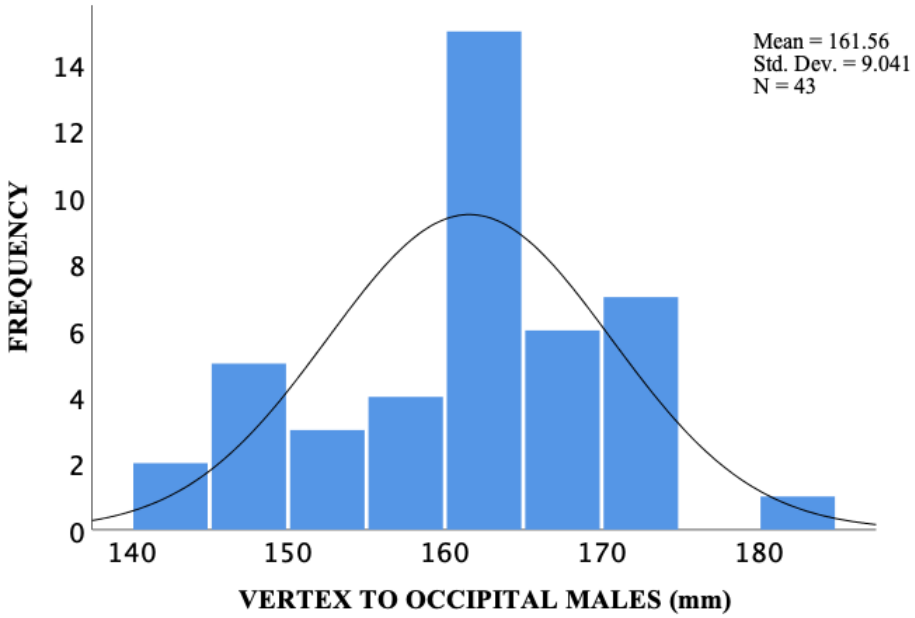

(b)

Figure 4.4. (a): Vertex to occipital protuberance measures' frequency histogram for females (n=69). (b): Vertex to occipital protuberance measure's frequency histogram for males (n=43).

Height Findings

The present height measures consisted of 60 participants. The mean height was 169.63 ± 9.90 cm (range 149 to 160 cm) (see Table 4.4). Males (174.95 ± 8.32 cm, range 156 to 190 cm) were taller than females (166.25 ± 9.70 cm, range 149 to 188 cm) (see figure 4.5.). The differences for males versus females heights were statistically significant [(t (58)= -3.563, p= 0.01].

Table 4.4. Heights distrubution of the participants (n=60) between genders.

		Mean	Sd	Min	Max
Height (cm)	**F (n=37)**	166.25	9.70	149	188
	M (n=23)	174.95	8.32	156	190
	Total (n=60)	169.63	9.90	149	190

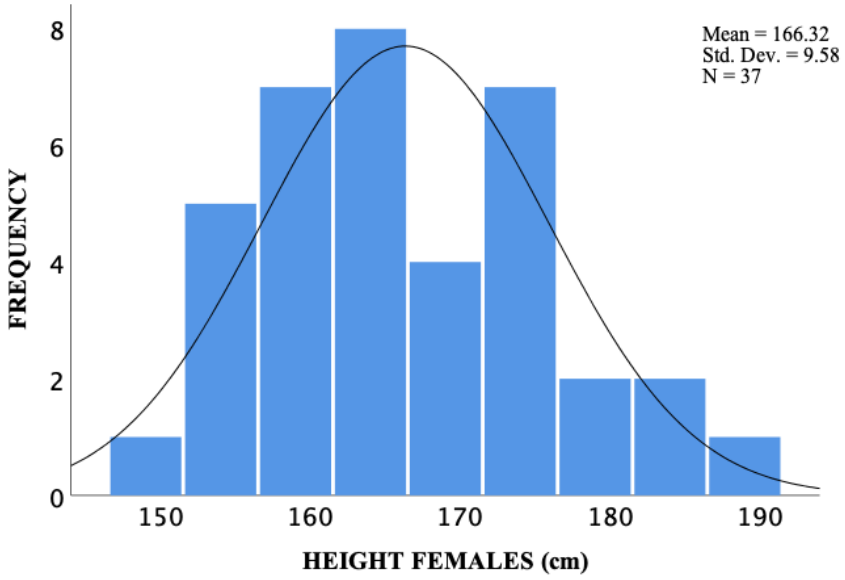

(a)

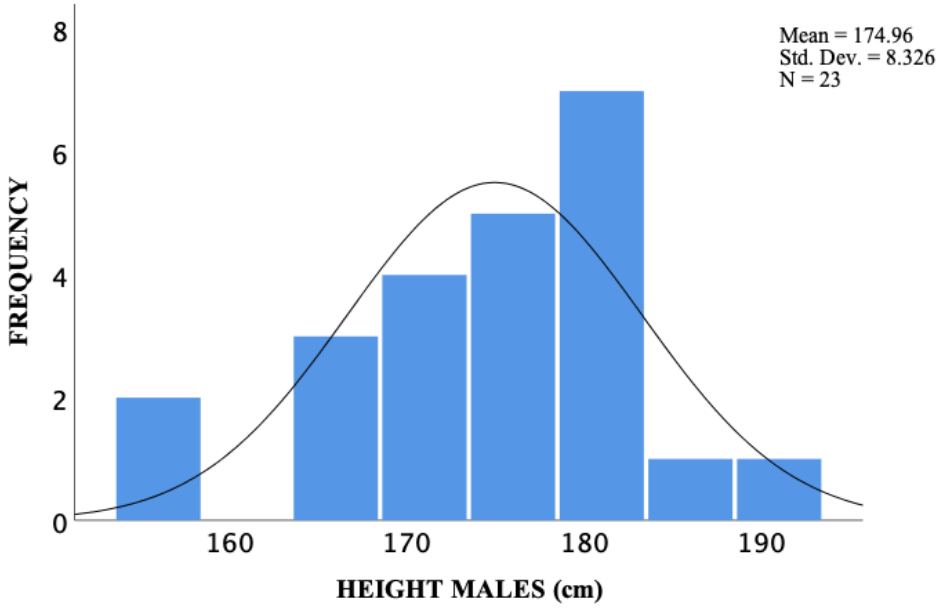

(b)

Figure 4.5. (a): The frequency histogram for height in females (n= 37). (b): The frequency histogram for height in males (n= 23).

Relationships of CDL, Head Size, and Height

CDL findings did not reveal any statistically significant correlations with present head size measures (see Table 4.5.). Figure 4.2. represented individual CDL outcomes in relation to vertex to occipital protuberance (r= 0.14, p= 0.154).

Table 4.5. Head size measures correlations with CDLs.

	CDL	
Right - Left pretragus (mm)	r= 0.01	p= 0.922
Left suborbital - Occipital (mm)	r= 0.09	p= 0.349
Right suborbital - Occipital (mm)	r= 0.11	p= 0.263
Left SSC - Right SSC (mm)	r= 0.03	p= 0.789
Vertex - Left pretragus (mm)	r= 0.10	p= 0.292
Vertex - Right pretragus (mm)	r= 0.10	p= 0.315
Vertex - Left SSC (mm)	r= 0.10	p= 0.291
Vertex - Right SSC (mm)	r= 0.11	p= 0.228
Occipital - Vertex (mm)	r= 0.14	p= 0.156
Left Carotid A. - Left Suborbital (mm)	r= 0.02	p= 0.854
Right Carotid A. - Right Suborbital (mm)	r= 0.02	p= 0.798

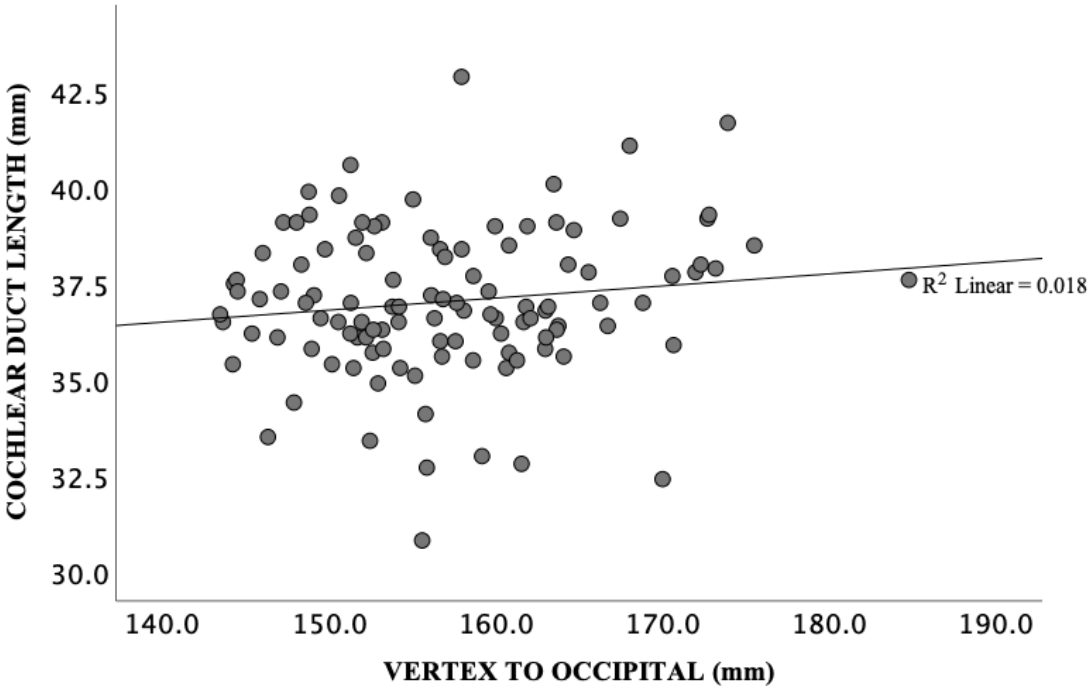

Figure 4.6. CDL was not significantly correlated with head size measures. The scatter graph demonstrated that the CDL correlations with vertex to occipital protuberance (r= 0.14, p= 0.156).

On the other hand, there were weak positive correlations between CDL and height (r= 0.25, p= 0.04) (see figure 4.7.). CDLs tended to be longer with the increase in height.

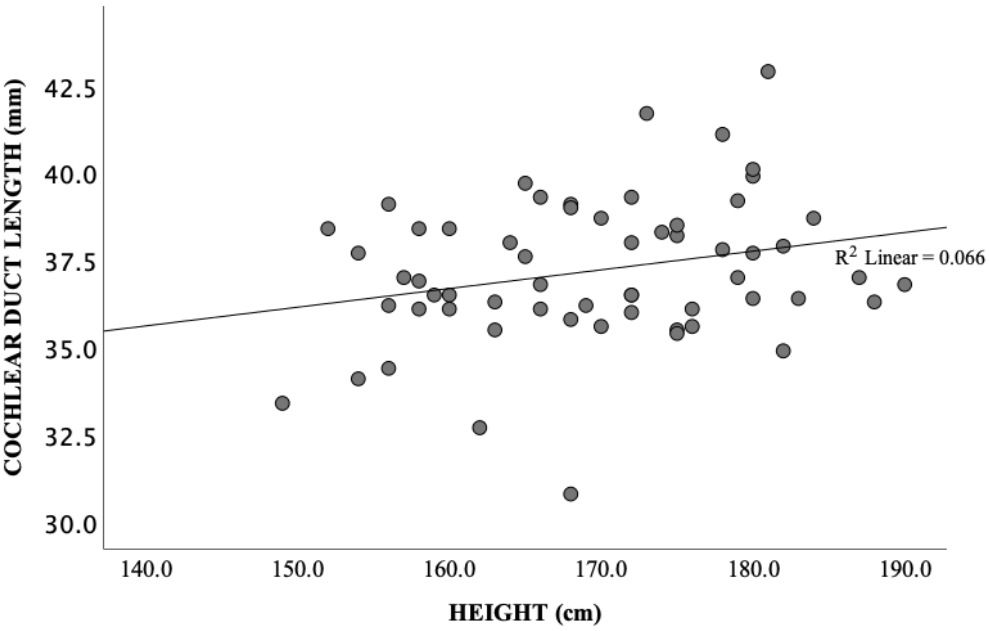

Figure 4.7. The scatter plots revealed significant positive weak correlations between CDL and height of participants (n=60, r= 0.25, p= 0.04).

To determine the effects of gender, CDL correlations with height were investigated separately for each gender subgroup. Gender-specific results did not show any statistically significant correlations between the CDL and height, reflecting significant effects of gender on both measures (females n=37, r= 0.17, p= 0.308; males n=23, r= 0.07, p= 0.743) (see figure 4.8.).

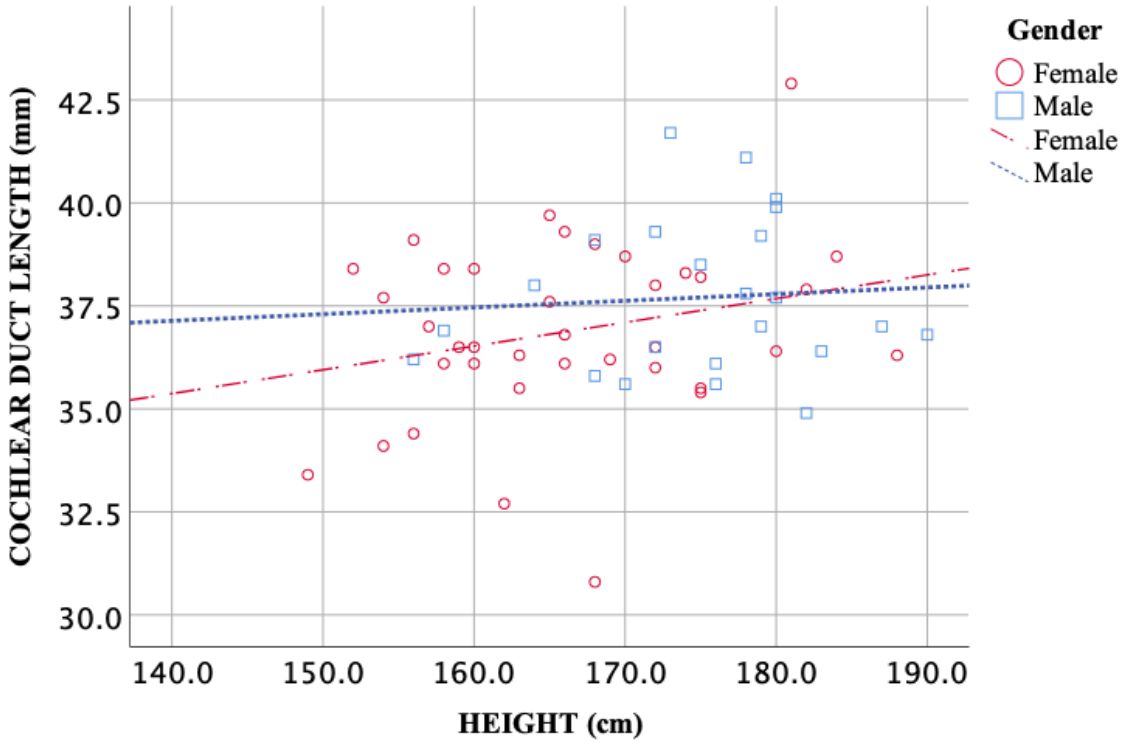

Figure 4.8. CDL relations with height in males and females. There were no statistically significant correlations between CDL and height in gender subgroups (female: n=37, r= 0.17, p= 0.38; male n=23, r= 0.07, p= 0.743).

Finally, there was a statistically significant positive correlation between head size and height (see Table 4.6.). Hence, head size tended to grow with the increase in height. The significant correlation coefficients between height and head size measures ranged from 0.29 to 0.48 ($p < 0.05$).

Table 4.6. Head size measures correlations with height.

	Height	
Right - Left pretragus (mm)	r= 0.34**	p= 0.007
Left suborbital - Occipital (mm)	r= 0.42**	p= 0.001
Right suborbital - Occipital (mm)	r= 0.45**	p< 0.001
Left SSC - Right SSC (mm)	r= 0.39**	p= 0.002
Vertex - Left pretragus (mm)	r= 0.38**	p= 0.002
Vertex - Right pretragus (mm)	r= 0.43**	p< 0.001
Vertex - Left SSC (mm)	r= 0.44**	p< 0.001
Vertex - Right SSC (mm)	r= 0.48**	P< 0.001
Occipital - Vertex (mm)	r= 0.39**	p= 0.002
Left Carotid A. - Left Suborbital (mm)	r= 0.29*	p= 0.021
Right Carotid A. - Right Suborbital (mm)	r= 0.35**	p= 0.005

**: Correlations were statistically significant at the p= 0.01 level, *: Correlations were statistically significant at the p= 0.05 level.

5. DISCUSSION

This study assessed the relationships of CDL with head size and body height. Previous studies have shown that cochlear shape was significantly affected by spatial restrictions around the cochlea (4). In the present study, it was hypothesized that the CDLs were significantly affected by surrounding structures during ontogenesis. Such anatomical characteristics might be preserved in the anatomy of the head. The results, while observing significant variations in individual CDL did not support the hypothesis: individual CDLs had no statistically significant correlations with head size measures. However, CDL showed weak correlations with body height.

The present outcomes are not affected by imprecise measurements. As can be seen in Fig. 4.2, measurement noise may contribute maximally to < 1.3% of the variability of our outcome measures, much more than the range of values of interest. This is thus insufficient to explain the absence of significant correlations. The absence of correlations thus suggests that there is no relation between the adult head size and the CDL.

However, both head size and CDL showed significant variability, as in previous studies. In the present study, CDL findings (mean= 37.04 ± 1.91 mm) were similar to those from Breitsprecher's study (mean= 37.0 ± 1.3 mm) using the same imaging technique (150). The CDL of the left and right cochlea did not differ significantly in the present study, consistently with many previous studies (27,102,151). Only, Thong et al.'s study (16) found that the basal turn length of the cochlea could differ between the two ears. The basal turn length is related to whether the cochlea has a wider or narrower basal and is affected by hearing loss and its degree (152–154). The reason for the difference found in Thong et al. (16)'s study between the two ears may be the degree of hearing loss.

As mentioned before, the cochlea does not continue to grow after birth and becomes mature at 17-19 WG. Therefore, in the present study, age did not show any significant effects on CDLs. Such results are in line with Waldeck et al., Würfel et al. and Pelliccia et al.'s findings (27,154,155). In addition, Pelliccia et al. did not observe any relationship between the age of the patients and height, basal turn length, and volume of the cochlea as well (154). Indeed, to the best of our knowledge, the unique study indicating a significant effect of age on CDLs is the one conducted by Hardy

(25) where the study findings reveal significant cochlear length differences between younger (<20 years old) and older (>40 years old) participants. However, the study consists of a relatively small and heterogeneous sample with a remarkable inequality of gender distribution for age subgroups of comparison. These might have caused these differences.

The significant effects of gender have been confirmed by the majority of existing studies, reflecting slightly longer mean CDLs in males (7,16,25,106,156). Conversely, many studies are showing no significant differences between female and male CDLs, similar to the present study (157–162). Such findings might partly be explained by the smaller sample size in comparison to some previous studies indicating significant gender effects (7,16,25,106,156).

With the different periods, the skull bones continue to grow after birth. Cochlea's surrounding structures such as the facial nerve differentiate in parallel with the eighth cranial nerve during the 3 WG (163). The facial nerve divide continues ventrally and the roots pass into the internal acoustic canal, where they join (164). In the development of the ear region, three stages can be differentiated: a blastemal period in E 20, when mesenchymal tissue surrounds ear structures; a cartilaginous period in 7 WG, when condensations of mesenchyme transform into a cartilaginous otic capsule; then an osseous period, when bone replaces cartilage (165). The shift from mesenchyme to cartilage, and then from cartilage to bone, is slow, thus one stage overlaps the next. However, before being constrained by surrounding cartilage and bone, the blastemal phase establishes the majority of the definite course of the facial nerve which is cause spatial constraints around the cochlea. The inner ear has almost completed its shape and is covered by cartilage at the end of the E 57 (166). By this phase, the majority of the definitive nerve route has been developed. The facial nerve has completed its development at E 58 with its route in the internal auditory canal. That is, the cochlea fully matures before the facial nerve takes its final form. Even in seemingly normal-appearing ears, the facial nerve route across the area varies considerably because facial nerve turns have a wide curve with various angles that display a wide range of sizes, from short to very large (150). The sequence in which inner ear components arise may have a significant impact on the nerve's final arrangement. The inner ear structures may affect shapes each other prenatally: for

example, Pietsch et al. (4) found that cochlear indentation where the facial nerve approaches the cochlear base. The cochlea's spiral shape has formed to provide a more effective packaging in the area where it is located (111). While there are standardized test subjects such as the mastoid, facial nerve, cochlear morphology, and the bone labyrinth capsule; anatomic evaluation of the cochlear dimensions is not conducted routinely before the surgery. Unfortunately, the present measurements were taken in the adult head, and this continues to grow substantially after birth. Since the final shape of the cochlea is established during intrauterine development, the adult condition may not be proportional to the condition during the development of the cochlea.

Head size is routinely measured as it is important for children's development therefore previous studies generally include the pediatric group's head circumference (22,68,69), in contrast to the adult group MR images in the present study. Marcus et al. (94) measured linear length between vertex to occipital points by CT as 128.94 mm in the pediatric population and in the present study linear length between occipital protuberance to vertex points has been found as 157.11 mm in an adult population. It is reasonable because the head size of the children is quite smaller than adults and continues to grow until 20 years old. On the other hand, Lin et al. (167) measured the linear length of the adult head's nasion to ophisthocranion points as 186.4 in males versus 176.0 in females and it's quite similar to the present study's left-suborbital-to-occipital measurement (mean= 188.16 mm in males versus 177.32 mm in females) as well as with the right-suborbital-to-occipital measurement (mean= 187.96 mm in males versus 177.10 mm in females). Although there were different landmarks in the present study, the linear distance from the nasion-to- ophisthocranion points seems spatially similar to the linear distance from the suborbital-points-to-occipital points. In addition, the linear length of the eurion-to-eurion points was found 160.5 mm in males and 154.6 mm in females according to Lin et al. (167)'s study and it is similar to the present study's right-to-left-pretragus measurement findings as 157.76 mm in males however it is slightly more than for females (149.89 mm). Similarly, the linear distance from the eurion-to-eurion points seems spatially similar to the linear distance from the right-to-left-pretragus points when looking at the anterior view of the human skull. As a result, it's reasonable to expect similar results for all of the measures in Lin et al. (167)'s study and the present studies.

Farkas et al. (80) measured the linear length of the glabella-to-occipital points as 189.2 mm in males similar to the present study's left-suborbital-to-occipital measures as 188.16 mm in males however slightly more for females (182.7 mm) than the present study (177.32 mm). According to Farkas et al. (80) and Lin et al. (167)'s studies, some linear distances were found more than in the present study, especially for females. They used martin's pelvimeter in their measurements, and factors such as skin and adipose tissue may have been more impact on females compared to the MRI technique in the present study, and the result of these measurements may have been overestimated. On the other hand, other studies (94,168) also have shown a difference of approximately 10 mm between males and females for each of the head size measures and they are similar to the present study.

Kayış et al. (169) measured adult males' linear length of the right-to-left-pretragus as 151.0 mm and it was slightly less than the present study's same distance of 157.76 mm. This little discrepancy might be due to differences in identifying the pretragus landmarks. In the same study, the linear length of the glabella-to-occipital points was found as 187.1 mm, and the present study's linear length of the left-suborbital-to-occipital and right-suborbital-to-occipital points were measured similarly (187.96 mm and 188.16 mm respectively). As mentioned before, glabella-to-occipital points seem spatially similar to the linear distance from the suborbital-to-occipital points, so these measures are quite similar in males similar to Farkas et al.(80)'s findings.

In addition, Aoyagi et al. (168) found adults' linear length of the tragus-to-tragus points 152 mm in females and 160 mm in males. Their findings are similar to the present study's linear length of the left-to-right-pretragus points as 149.89 mm in females and 157.76 mm in males. The inter-tragus and inter-pretragus measures are similar in the lateral axis of the skull since they are adjacent landmarks. Likewise, Lacko et al. (170) found adults' tragus-to-tragus measures as 148 mm for both genders with 3D MRI scans, similar to the present study (152.56 mm). Although the head anthropometry studies mentioned before generally used Martin's Pelvimeter, it's quite similar to the present study's head size results which used 3D MRI scans.

Similar to the literature (18,168,171), the present study findings differ significantly between genders and show larger head size measures for the males than

those for the females. Contrary to expectation, however, there were no statistically significant correlations between present CDL and head size findings. The cochlea maturates prenatally whereas the head continues to grow until adolescence. This fact might be the underlying reason for such outcomes. Different factors may be involved in the growth of the head in the postnatal period. However, if the cochlear shape is investigated in detail i.e. cochlear turns with head size or cochlear volumes with the head size the differences might be observed in the microscopic plan. Growths in the basal and middle turn can be associated with the cochlear turns' space, for example, narrower basal turns and shorter preauricular distances. In individuals with a smaller head width, the cochlea may have a more spiral shape due to spatial restrictions however no change in CDL. Pietsch worked with micro-CT and specifically studied the cochlear shape. The structures surrounding the cochlea nearly have a significant effect on the cochlear shape. The CDL is found to be affected by different factors. In terms of study population features, Grover et al. (172) from India claimed that Asians had less CDL, conversely, Singla (173) et al. from India as well reported one of the longest CDL in the literature. Atalay et al. (174) studied CDL covariations of CDL, including gender, age, population characteristics, the origin of cochlear material, measured structure, and measurement method. The cochlear size was observed to be significantly shorter for individuals with congenital sensorineural hearing loss (CSNHL) but not for other covariations. Similarly, Grover et al. (172)’s study included children with CSNHL and they found shorter CDL in them than in previous studies. A problem during the formation of the basilar membrane may explain that the children with CSNHL have shorter CDL than the normal cochlea. In addition, Pelliccia et al. (154) investigated cochlear size variability among the degree of hearing loss in a total of 241 patients with both congenital and post-lingual hearing loss. The total length of the cochlea is unaffected by the degree of sensorineural hearing loss; however, it can impact the height and basal turn length of the cochlea. It is reasonable that post-lingual sensorineural hearing loss can’t have an effect on CDL that matures before birth. These results are similar to Lan et al.(152) and Purcell et al.(153)’s findings, which indicate that CSNHL affected the cochlea's height and basal turn length. The present study's participants were post-lingual deafened and the mean CDL is longer than CDL in CSNHL studies (159,172,175). As a result, CSNHL and shorter cochlea may share

the same etiological origin. The present study could not investigate CDL relationships with the auditory results due to missing audiological data, but this topic continues to be particularly very interesting for hearing impaired people with cochlear implants.

In the phylogenetic studies, Beals et al. (124) compared the CDL of the gorilla (36.32 mm), chimpanzees (35.88 mm), Neandertals (37.27 mm), and modern humans (36.62 mm) from cadaveric temporal bone specimens and they found that the mean CDL of four species were not statistically different, however, the number of cochlear turns was statistically different between these species. Additionally, they investigated cochlear volumes and Neandertal absolute cochlear volumes are in line with modern human cochlear volumes, but significantly larger than gorillas and chimpanzees' cochlear volumes. Cochlear shape reconstruction of these four species not only shows the similarities in shape but also differences. Cochlear volume may represent changes in the overall shape of the bone labyrinth (15) and its surrounding structures, whereas CDL reflects the similar total length of the basilar membrane between these species (117). It is known that Neandertals have significantly bigger and especially expanded skulls than modern humans but similar brain volumes (176–178). The gorillas have a larger head than humans, but conversely, smaller brains which is the result of the more flattened shape of the head (179). Chimpanzees have much smaller heads than humans (180). But these species' CDLs are similar to modern humans (121). And the result of this relationship suggests that the growths in the head in relative species mostly affect the shape of the cochlea, not comparable to CDL.

In another phylogenetic study, Ekdale et al. (129) found a significant correlation between the head length (range 543 -16.9 mm) and the bony labyrinth length (range 2.71 – 10.1 mm) of highly different several placental mammals ($r= 0.80$, $p< 0.01$). Although no comparable differences in CDL and head size could be found between related species or within the same species, a significant correlation is observed between very different taxes. Interindividual variability was not assessed.

On the other hand, the CDL of the present study is significantly correlated ($r= 0.24$, $p< 0.05$) with individual height although many factors affect height during the development process. The weak correlation and the absence of gender-specific correlation may indicate the presence of a correlation in the gender effect.

The height is also significantly correlated with head size measures. Mansur et al. (17) found a correlation between head circumference and individual height statistically significant ($r = 0.443$ for males, $r = 0.302$, $p<0.01$ for males and females). According to Hshieh et al. (18) coefficient factor for a significant correlation between head circumference and individual height was found as 0.46. In the present study, correlation coefficients ranged from 0.29-to 0.48 which is similar to previous studies' coefficients. The Head circumference measurement method was used in the past studies and even though a different method was used in this study; the correlation coefficients were found to be similar to the past studies.

Only the length of the cochlea was measured in the present study, but other important parameters such as height and basal turn length of the cochlea were not examined along with different head size measures. In the previous studies, CSNHL affected temporal bone structures such as the larger bony width of the semicircular canals and the height of the cochlea (152,153). Differences occur in the temporal bone during the development of the cochlea and CSNHL, which is hearing loss that occurs during the development, affects the cochlea. The width of the area in which the cochlea is located may cause at first subtle differences in the inner ear. Therefore, small differences in the cochlear shape may be investigated. However, this is the first study that gives an idea of how much the CDL is affected by external factors in maturational development. Although no relationship was found between CDL and head size in the study, the whole cochlea and the surrounding structures in the area are developing at around the same time in orthogenesis, so they may affect each other in this process. Further research may investigate the relationships between the structures in the temporal bone and the cochlea specifically during intrauterine development.

6. CONCLUSION AND RECOMMENDATIONS

The present study entitled 'The Relation Between Cochlear Duct Length and Head Size Assessed by MRI and CBCT is the first attempt to investigate the relationships between CDL, head size, and height in humans. Specifically, the cochlea and the head are thought to have significant correlations in size since the cochlea is developing in the temporal bone embedded in the head. For this purpose, CDLs assessed by CBCT were compared with head size landmarks assessed by MRI. Moreover, the effects of demographics such as age and gender were studied to understand the factors that may be affecting the CDL, head size, and height. In conclusion, the following findings had been observed:

1- The CDLs from the opposite ears were very similar and did not show any statistically significant differences.
2- As expected, the age did not show any statistically significant effects on the CDL.
3- The average CDL from males was remarkably longer than that of females but the gender differences did not achieve statistical significance.
4- The average head size measure was longer for males than that for females and the gender differences were statistically significant.
5- Similarly, with the head size, the males were taller than the females on average and these differences in height were statistically significant.
6- The CDL and the head size did not correlate significantly with each other.
7- The CDL and the height of individuals had significant but weak relationships.
8- Similar to the literature, the height and the head size showed statistically significant relationships with each other.

Based on these results, it can be concluded that the CDL relationships with head size are not statistically significant, on the other hand, the height has significant weak relationships. Despite sharing an interrelated genetic makeup, the head size and the height can be affected by other factors such as nutrition during the life course. However, the observation of gender differences showing similar tendencies towards shorter measures for females' CDL, head size, and height within the same sample highlights the need for further research. Rather than the length, the cochlear shape

might be affected by spatial restrictions. Indeed, the shape of the cochlea and the head, more specifically the surrounding structures of the cochlea, may share some similarities. Future research may focus on the relationships between the cochlear shape and its' surrounding structures by using micro-CT.

7. REFERENCES

1. Michael S, Erik S, Udo S, Brian M, Stefan C, Zeberg H. Atlas of Anatomy, Latin Nomenclature, 2nd edition. Three Volume Set. Thieme Medical Publishers; 2016, 1–1959.

2. Johnson Chacko L, Wertjanz D, Sergi C, et al. Growth and cellular patterning during fetal human inner ear development studied by a correlative imaging approach. BMC Dev Biol. 2019;19(1):11. doi:10.1186/s12861-019-0191-y.

3. Franke-Trieger A, Jolly C, Darbinjan A, Zahnert T, Mürbe D. Insertion depth angles of cochlear implant arrays with varying length: a temporal bone study. Otol Neurotol. 2014;35(1):58-63. doi:10.1097/MAO.0000000000000211.

4. Pietsch M, Aguirre Dávila L, Erfurt P, Avci E, Lenarz T, Kral A. Spiral Form of the Human Cochlea Results from Spatial Constraints. Sci Rep. 2018;8(1):7020.

5. Alexiades G, Dhanasingh A, Jolly C. Method to estimate the complete and two-turn cochlear duct length. Otol Neurotol. 2015;36(5):904-907. doi:10.1097/MAO.0000000000000620. 2015.

6. Erixon E, Högstorp H, Wadin K, Rask-Andersen H. Variational anatomy of the human cochlea: implications for cochlear implantation. Otol. Neurotol. 2009;30(1):14-22. doi:10.1097/MAO.0b013e31818a08e8.

7. Escudé B, James C, Deguine O, Cochard N, Eter E, Fraysse B. The size of the cochlea and predictions of insertion depth angles for cochlear implant electrodes. Audiol Neurootol. 2006;11. doi:10.1159/000095611.

8. Litovsky R. Development of the auditory system. Handb Clin Neurol. 2015;129:55-72. doi:10.1016/B978-0-444-62630-1.00003-2.

9. Avci E, Nauwelaers T, Lenarz T, Hamacher V, Kral A. Variations in microanatomy of the human cochlea. J Comp Neurol. 2014;522(14):3245-3261. doi:10.1002/cne.23594.

10. D'Arcy W, Thompson. On growth and form. Vol. 2. Cambridge: Cambridge university press; 1961.

11. Kuthubutheen J, Grewal A, Symons S, et al. The Effect of Cochlear Size on Cochlear Implantation Outcomes. Biomed Res Int. 2019;2019:5849871. doi:10.1155/2019/5849871.

12. Ekdale EG. Form and function of the mammalian inner ear. J Anat. 2016;228(2):324-337. doi:10.1111/joa.12308.

13. Landsberger DM, Svrakic M, Roland JT Jr, Svirsky M. The Relationship Between Insertion Angles, Default Frequency Allocations, and Spiral Ganglion Place Pitch in Cochlear Implants. Ear Hear. 2015;36(5):e207-e213. doi:10.1097/AUD.0000000000000163.

14. Heutink F, de Rijk SR, Verbist BM, Huinck WJ, Mylanus EAM. Angular Electrode Insertion Depth and Speech Perception in Adults With a Cochlear Implant: A Systematic Review. Otol Neurotol. 2019;40(7):900-910. doi:10.1097/MAO.0000000000002298.

15. Manoussaki D, Dimitriadis EK, Chadwick RS. Cochlea's graded curvature effect on low frequency waves. Phys Rev Lett. 2006;96(8):088701. doi:10.1103/PhysRevLett.96.088701.

16. Thong JF, Low D, Tham A, Liew C, Tan TY, Yuen HW. Cochlear duct length-one size fits all?. Am J Otolaryngol. 2017;38(2):218-221. doi:10.1016/j.amjoto.2017.01.015.

17. Mansur D. I, Haque MK, Sharma K, Mehta DK, Shakya R. Use of head circumference as a predictor of height of individual. Kathmandu Univ Med J. 2014;12(2), 89-92.

18. Hshieh TT, Fox ML, Kosar CM, et al. Head circumference as a useful surrogate for intracranial volume in older adults. Int Psychogeriatr. 2016;28(1):157-162. doi:10.1017/S104161021500037X.

19. Heutinck P, Knoops P, Florez NR, et al. Statistical shape modelling for the analysis of head shape variations. J Craniomaxillofac Surg. 2021;49(6):449-455. doi:10.1016/j.jcms.2021.02.020.

20. Weech AA. Signposts on the highway of growth. AMA Am J Dis Child. 1954;88(4):452-457. doi:10.1001/archpedi.1954.02050100454004.

21. Haworth S, Shapland CY, Hayward C, et al. Low-frequency variation in TP53 has large effects on head circumference and intracranial volume. Nat Commun. 2019;10(1):357. doi:10.1038/s41467-018-07863-x.

22. Rau A, Demerath T, Kremers N, Eckenweiler M, von der Warth R, Urbach H. Measuring the Head Circumference on MRI in Children: an Interrater Study. Clin Neuroradiol. 2021;31(4):1021-1027. doi:10.1007/s00062-021-01019-z.

23. Møller, Aage R. Hearing: anatomy, physiology, and disorders of the auditory system. Plural Publishing, Texas; 2012.

24. Frank EM, Baran AJ. The auditory system: Anatomy, physiology, and clinical correlates. Plural Publishing; 2018.

25. Hardy, M., The length of the organ of Corti in man. Am. J. Anat. 1938;62(1): 291-311. https://doi.org/10.1002/aja.1000620204.

26. Kawano A, Seldon HL, Clark GM. Computer-aided three-dimensional reconstruction in human cochlear maps: measurement of the lengths of organ of Corti, outer wall, inner wall, and Rosenthal's canal. Ann Otol Rhinol Laryngol. 1996;105(9):701-709. doi:10.1177/000348949610500906.

27. Würfel W, Lanfermann H, Lenarz T, Majdani O. Cochlear length determination using Cone Beam Computed Tomography in a clinical setting. Hear Res. 2014;316:65-72. doi:10.1016/j.heares.2014.07.013.

28. Ades HW, Axelsson A, Baird IL, v. Békésy G, Boord RL, Campbell CBG, et al. Anatomical features of the inner ear in submammalian vertebrates, Auditory System. Springer, Berlin, Heidelberg, 1974. p. 159-212.

29. Carpenter RHS. Mammalian vestibular physiology. Nature. 1980,284(5755):494-494.

30. Tascioglu AB. Brief review of vestibular system anatomy and its higher order projections. Neuroanatomy, 2005, 4.4: 24-27.

31. Leonetti JP, Smith PG, Linthicum FH. The petrous carotid artery: anatomic relationships in skull base surgery. Otolaryngol Head Neck Surg. 1990;102(1):3-12. doi:10.1177/019459989010200102.

32. Scarabino T, Salvolini U. Atlas of morphology anf functional anatomy of the brain. Springer, Verlag, Berlin, Heidelberg; 2006.

33. Harrison, Robert V. The biology of hearing and deafness. Charles C. Thomas Publisher; 1988.

34. Elverland HH. Ascending and intrinsic projections of the superior olivary complex in the cat. Exp Brain Res. 1978;32(1):117-134. doi:10.1007/BF00237396.

35. Brodal A. Neurological anatomy, Relation to Clinical Anatomy. Annals of Neurology. 1981;10(6).

36. Fay RR, Popper AN. The lateral line system New York, Springer; 2014.

37. Roberson GH. Diagnostic and Surgical Imaging Anatomy: Brain, Head & Neck, Spine. 2007. American Journal of Roentgenology. 2007 Jan;188(1).

38. Talavage TM, Sereno MI, Melcher JR, Ledden PJ, Rosen BR, Dale AM. Tonotopic organization in human auditory cortex revealed by progressions of frequency sensitivity. J Neurophysiol. 2004;91(3):1282-1296. doi:10.1152/jn.01125.2002.

39. Jutras B, Lagacé J, Koravand A. The development of auditory functions. Handb Clin Neurol. 2020;173:143-155. doi:10.1016/B978-0-444-64150-2.00014-9.

40. Moore JK, Linthicum FH Jr. The human auditory system: a timeline of development. Int J Audiol. 2007;46(9):460-478. doi:10.1080/14992020701383019.

41. Northern J, Downs M. What is hearing loss. Hearing in Children. 1984;3(1):21.

42. Keefe DH, Bulen JC, Arehart KH, Burns EM. Ear-canal impedance and reflection coefficient in human infants and adults. J Acoust Soc Am. 1993;94(5):2617-2638. doi:10.1121/1.407347.

43. Holborow C. Eustachian tubal function. Changes in anatomy and function with age and the relationship of these changes to aural pathology. Arch Otolaryngol. 1970;92(6):624-626. doi:10.1001/archotol.1970.04310060096017.

44. Kitajiri M, Sando I, Takahara T. Postnatal development of the eustachian tube and its surrounding structures. Preliminary study. Ann Otol Rhinol Laryngol. 1987;96(2 Pt 1):191-198. doi:10.1177/000348948709600211.

45. Ishijima K, Sando I, Balaban C, Suzuki C, Takasaki K. Length of the eustachian tube and its postnatal development: computer-aided three-dimensional reconstruction and measurement study. Ann Otol Rhinol Laryngol. 2000;109(6):542-548. doi:10.1177/000348940010900603.

46. Helwany M, Tadi P. Embryology, Ear. Treasure Island (FL): StatPearls Publishing; 2021.

47. Rubel EW, Fritzsch B. Auditory system development: primary auditory neurons and their targets. Annu Rev Neurosci. 2002;25:51-101. doi:10.1146/annurev.neuro.25.112701.142849.

48. Luo ZX, Ruf I, Schultz JA, Martin T. Fossil evidence on evolution of inner ear cochlea in Jurassic mammals. Proc Biol Sci. 2011;278(1702):28-34. doi:10.1098/rspb.2010.1148.

49. Raft S, Nowotschin S, Liao J, Morrow BE. Suppression of neural fate and control of inner ear morphogenesis by Tbx1. Development. 2004;131(8):1801-1812. doi:10.1242/dev.01067.

50. Jeffery N, Spoor F. Prenatal growth and development of the modern human labyrinth. J Anat. 2004;204(2):71-92. doi:10.1111/j.1469-7580.2004.00250.x.

51. Wu DK, Kelley MW. Molecular mechanisms of inner ear development. Cold Spring Harb Perspect Biol. 2012;4(8):a008409. doi:10.1101/cshperspect.a008409.

52. Abdala C, Keefee DH, Douglas H. Morphological and functional ear development. Human auditory development. Springer, New York, NY; 2012, p. 19-59.

53. Kacker SK, Deka RC. Auditory brainstem evoked responses in meniere's disease. Indian Journal of Otolaryngology. 1986;38(1):14-17.

54. Eggermont JJ, Moore JK. Morphological and functional development of the auditory nervous system. Human auditory development. Springer, New York; 2012, p. 61-105.

55. Raininko R, Autti T, Vanhanen SL, Ylikoski A, Erkinjuntti T, Santavuori P. The normal brain stem from infancy to old age. A morphometric MRI study. Neuroradiology. 1994;36(5):364-368. doi:10.1007/BF00612119.

56. Stiles J, Jernigan TL. The basics of brain development. Neuropsychol Rev. 2010;20(4):327-348. doi:10.1007/s11065-010-9148-4.

57. Blakemore SJ. Development of the social brain in adolescence. J R Soc Med. 2012;105(3):111-116. doi:10.1258/jrsm.2011.110221.

58. Lenroot RK, Giedd JN. Brain development in children and adolescents: insights from anatomical magnetic resonance imaging. Neurosci Biobehav Rev. 2006;30(6):718-729. doi:10.1016/j.neubiorev.2006.06.001.

59. Wang YX. Advances in Experimental Medicine and Biology Preface; 2017, p. 967.

60. Barbara SC, Leonard V, Le W, Hari B. Individual differences in temporal perception and their implications for everyday listening. The Frequency-Following Response, Springer; 2017, p. 159-192.

61. Harold FS, Aina JG. Anatomy of the temporal bone with surgical implications. Lea & Febiger, 3rd edition; 1986.

62. Winckler JR, et al. New high-resolution ground-based studies of sprites. Journal of Geophysical Research: Atmospheres, Wiley; 1996.

63. Tomohito N, Yoshinori K. Using the petrous part of the temporal bone to estimate fetal age at death. Forensic Science International, Elsevier; 2015.

64. Stuart HC, Stevenson SS. In Mitchell-Nelson Textbook of Pediatrics, Saunders; 1950.

65. Krogman WM, Johnston FE. The physical growth of Philadelphia white children, age 7-17 years. Philadelphia Center for Research in Child Growth; 1965.

66. Krogman WM. Height, weight and bodily growth of American white and American Negro boys and girls of Philadelphia, age 6-14 years. Philadelphia Center for Research in Child Growth; 1960.

67. Meyer-Marcotty P, Böhm H, Linz C, Kochel J, Stellzig-Eisenhauer A, Schweitzer T. Three-dimensional analysis of cranial growth from 6 to 12 months of age. Eur J Orthod. 2014;36(5):489-496. doi:10.1093/ejo/cjt010.

68. Swearingen JJ, Joseph WY. Determination of centers of gravity of children, sitting and standing. Federal Aviation Agency, Office of Aviation Medicine; 1965.

69. Huelke DF. An overview of anatomical considerations of infants and children in the adult world of automobile safety design. Annual Proceedings/Association for the Advancement of Automotive Medicine, Vol. 42;1998, p. 93.

70. Henry M, J Parsons S. Morris' Human Anatomy: A Complete Systematic Treatise. P. Blakiston's Son & Company; 1925.

71. Manzanares MC, Goret-Nicaise M, Dhem A. Metopic sutural closure in the human skull. J Anat. 1988;161:203-215. J Anat.

72. Chopra SRK. The cranial suture closure in monkeys. Proceedings of the Zoological Society of London. Vol. 128. Blackwell Publishing, Oxford, UK; 1957; p. 67-112.

73. Cohen MM Jr. Sutural biology and the correlates of craniosynostosis. Am J Med Genet. 1993;47(5):581-616. doi:10.1002/ajmg.1320470507.

74. Voigt M, Meyer-Kahrweg LM, Landau-Crangle E, et al. Individualized birth length and head circumference percentile charts based on maternal body weight and height. J Perinat Med. 2020;48(7):656-664. doi:10.1515/jpm-2020-0085. Journal of Perinatal Medicine. 2020 Sep 1;48(7):656–64.

75. Baum JD, Searls D. Head shape and size of pre-term low-birthweight infants. Dev Med Child Neurol. 1971;13(5):576-581. doi:10.1111/j.1469-8749.1971.tb08320.x. Vol. 13.

76. Human Phenotypes [Internet]. 2018 [Date of Access 10.02.2022]. Access adress: http://humanphenotypes.net/metrics/heightlengthindex.html.

77. Bunak V. Metodika antropometricheskih issledovanij [Method of anthropometric studies]. Gosmedizdat, Moscow; 1931, p. 168.

78. Vishal MS, Chikatapu C. The Study Of Vertical Cephalic Index (Length-Height Index) And Transverse Cephalic Index (Breadth-Height Index) Of Andhra Region (India). Asian Journal of Medical Sciences. 2012;3(3):6-11.

79. Gentry S, Claud AB. The anatomy and biology of the human skeleton. Texas A&M University Press; 1988.

80. Farkas LG, Posnick JC, Hreczko TM. Anthropometric growth study of the head. Cleft Palate Craniofac J. 1992;29(4):303-308. doi:10.1597/1545-1569_1992_029_0303_agsoth_2.3.co_2.

81. Martini M, Klausing A, Lüchters G, Heim N, Messing-Jünger M. Head circumference - a useful single parameter for skull volume development in cranial growth analysis?. Head Face Med. 2018;14(1):3.

82. Bushby KM, Cole T, Matthews JN, Goodship JA. Centiles for adult head circumference. Arch Dis Child. 1992;67(10):1286-1287. doi:10.1136/adc.67.10.1286.

83. Smit DJ, Luciano M, Bartels M, et al. Heritability of head size in Dutch and Australian twin families at ages 0-50 years. Twin Res Hum Genet. 2010;13(4):370-380. doi:10.1375/twin.13.4.370.

84. Ahmet RÖ, Gürbüz H, Ayata A, Çetin H. Adult head circumferences and centiles. Journal of Turgut Ozal Medical Center. 1997;4(3):261-264.

85. Kamdar MR, Gomez RA, Ascherman JA. Intracranial volumes in a large series of healthy children. Plast Reconstr Surg. 2009;124(6):2072-2075. doi:10.1097/PRS.0b013e3181bcefc4.

86. Falk D, Hildebolt C, Smith K, et al. LB1's virtual endocast, microcephaly, and hominin brain evolution. J Hum Evol. 2009;57(5):597-607. doi:10.1016/j.jhevol.2008.10.008.

87. Vannucci RC, Barron TF, Lerro D, Antón SC, Vannucci SJ. Craniometric measures during development using MRI. Neuroimage. 2011;56(4):1855-1864. doi:10.1016/j.neuroimage.2011.03.044.

88. Cooke RW, Lucas A, Yudkin PL, Pryse-Davies J. Head circumference as an index of brain weight in the fetus and newborn. Early Hum Dev. 1977;1(2):145-149. doi:10.1016/0378-3782(77)90015-9.

89. Bartholomeusz HH, Courchesne E, Karns CM. Relationship between head circumference and brain volume in healthy normal toddlers, children, and adults. Neuropediatrics. 2002;33(5):239-241. doi:10.1055/s-2002-36735.

90. Sgouros S, Goldin JH, Hockley AD, Wake MJ, Natarajan K. Intracranial volume change in childhood. J Neurosurg. 1999;91(4):610-616. doi:10.3171/jns.1999.91.4.0610.

91. Smith K, Politte D, Reiker G, et al. Automated measurement of skull circumference, cranial index, and braincase volume from pediatric computed tomography. Annu Int Conf IEEE Eng Med Biol Soc. 2013;2013:3977-3980. doi:10.1109/EMBC.2013.6610416.

92. Seeberger R, Hoffmann J, Freudlsperger C, et al. Intracranial volume (ICV) in isolated sagittal craniosynostosis measured by 3D photocephalometry: A new perspective on a controversial issue. J Craniomaxillofac Surg. 2016;44(5):626-631. doi:10.1016/j.jcms.2016.01.023.

93. Kyriakopoulou V, Vatansever D, Davidson A. Normative biometry of the fetal brain using magnetic resonance imaging. Brain Struct Funct. 2017;222(5):2295-2307. doi:10.1007/s00429-016-1342-6.

94. Marcus JR, Domeshek LF, Das R, et al. Objective three-dimensional analysis of cranial morphology. Eplasty. 2008;8:e20.

95. Vannucci RC, Barron TF, Lerro D, Antón SC, Vannucci SJ. Craniometric measures during development using MRI. Neuroimage. 2011;56(4):1855-1864. doi:10.1016/j.neuroimage.2011.03.044.

96. Yepes-Calderon F, Wihardja F, Sloan A, Kim J, Nelson MD, McComb JG. Measuring Maximum Head Circumference Within the Picture Archiving and Communication

System: A Fully Automatic Approach. Front Pediatr. 2021;9:608122. doi:10.3389/fped.2021.608122.

97. Koch RW, Ladak HM, Elfarnawany M, Agrawal SK. Measuring Cochlear Duct Length - a historical analysis of methods and results. J Otolaryngol Head Neck Surg. 2017;46(1):19. doi:10.1186/s40463-017-0194-2.

98. Ulehlová L, Voldrich L, Janisch R. Correlative study of sensory cell density and cochlear length in humans. Hear Res. 1987;28(2-3):149-151. doi:10.1016/0378-5955(87)90045-1.

99. Ketten DR, Skinner MW, Wang G, Vannier MW, Gates GA, Neely JG. In vivo measures of cochlear length and insertion depth of nucleus cochlear implant electrode arrays. Ann Otol Rhinol Laryngol Suppl. 1998;175:1-16.

100. Dimopoulos P, Muren C. Anatomic variations of the cochlea and relations to other temporal bone structures. Acta Radiol. 1990;31(5):439-444.

101. Mistrík P, Jolly C. Optimal electrode length to match patient specific cochlear anatomy. Eur Ann Otorhinolaryngol Head Neck Dis. 2016;133 Suppl 1:S68-S71. doi:10.1016/j.anorl.2016.05.001.

102. Hochmair I, Hochmair E, Nopp P, Waller M, Jolly C. Deep electrode insertion and sound coding in cochlear implants. Hear Res. 2015;322:14-23. doi:10.1016/j.heares.2014.10.006.

103. Kiefer J, Pok M, Adunka O, et al. Combined electric and acoustic stimulation of the auditory system: results of a clinical study. Audiol Neurootol. 2005;10(3):134-144. doi:10.1159/000084023.

104. Gstoettner W, Kiefer J, Baumgartner WD, Pok S, Peters S, Adunka O. Hearing preservation in cochlear implantation for electric acoustic stimulation. Acta Otolaryngol. 2004;124(4):348-352. doi:10.1080/00016480410016432.

105. Braun K, Böhnke F, Stark T. Three-dimensional representation of the human cochlea using micro-computed tomography data: presenting an anatomical model for further numerical calculations. Acta Otolaryngol. 2012;132(6):603-613. doi:10.3109/00016489.2011.653670.

106. Meng J, Li S, Zhang F, Li Q, Qin Z. Cochlear size and shape variability and implications in cochlear implantation surgery. Otology and Neurotology. 2016;37(9):1307–13.

107. Elfarnawany M, Alam SR, Rohani SA, Zhu N, Agrawal SK, Ladak HM. Micro-CT versus synchrotron radiation phase contrast imaging of human cochlea. J Microsc. 2017;265(3):349-357. doi:10.1111/jmi.12507.

108. Helpard L, Li H, Rask-Andersen H, Ladak HM, Agrawal SK. Characterization of the human helicotrema: implications for cochlear duct length and frequency mapping. J Otolaryngol Head Neck Surg. 2020;49(1):2. Published 2020 Jan 6. doi:10.1186/s40463-019-0398-8.

109. Wright A, Davis A, Bredberg G, et al. Hair cell distributions in the normal human cochlea. A report of a European working group. Acta Otolaryngol Suppl. 1987;436:15-24. doi:10.3109/00016488709124972.

110. Guild SR. A graphic reconstruction method for the study of the organ of Corti. Anat Rec. 1921;22:140-157.

111. Gulya AJ. Anatomy of the temporal bone with surgical implications. CRC Press; 2007.

112. Takagi A, Sando I. Computer-aided three-dimensional reconstruction: a method of measuring temporal bone structures including the length of the cochlea. Ann Otol Rhinol Laryngol. 1989;98(7 Pt 1):515-522. doi:10.1177/000348948909800705.

113. Schurzig D, Pietsch M, Erfurt P, Timm ME, Lenarz T, Kral A. A cochlear scaling model for accurate anatomy evaluation and frequency allocation in cochlear implantation. Hear Res. 2021;403:108166. doi:10.1016/j.heares.2020.108166.

114. Armstrong SD, Bloch JI, Houde P, Silcox MT. Cochlear labyrinth volume in euarchontoglirans: implications for the evolution of hearing in primates. Anat Rec (Hoboken). 2011;294(2):263-266. doi:10.1002/ar.21298.

115. Makishima T, Hochman L, Armstrong P, et al. Inner ear dysfunction in caspase-3 deficient mice. BMC Neurosci. 2011;12:102. Published 2011 Oct 12. doi:10.1186/1471-2202-12-102.

116. Coleman MN, Colbert MW. Correlations between auditory structures and hearing sensitivity in non-human primates. J Morphol. 2010;271(5):511-532. doi:10.1002/jmor.10814.

117. West CD. The relationship of the spiral turns of the cochlea and the length of the basilar membrane to the range of audible frequencies in ground dwelling mammals. J Acoust Soc Am. 1985;77(3):1091-1101. doi:10.1121/1.392227.

118. Kirk EC, Gosselin-Ildari AD. Cochlear labyrinth volume and hearing abilities in primates. Anat Rec (Hoboken). 2009;292(6):765-776. doi:10.1002/ar.20907.

119. Douglas W, Darlene RK. Marine mammal sensory systems. Biology of marine mammals; 1999, p. 117-175.

120. Echteler SM, Richard RF, Popper NA. Structure of the mammalian cochlea. Comparative hearing: mammals. Springer, New York; 1994, p. 134-171.

121. Gerald F. Hearing in extinct cetaceans as determined by cochlear structure. Journal of Paleontology, JSTOR; 1976, p. 133-152.

122. Geisler JH, Luo Z. The petrosal and inner ear of Herpetocetus (Mammalia: Cetacea) and their implications for the phylogeny and hearing of archaic mysticetes. Journal of Paleontology. 1996;70(6):1045-1066.

123. Eric GE, Timothy R. Morphology and variation within the bony labyrinth of zhelestids (Mammalia, Eutheria) and other therian mammals. Journal of Vertebrate Paleontology. 2011;31(3):658-675.

124. Beals ME, Frayer DW, Radovčić J, Hill CA. Cochlear labyrinth volume in Krapina Neandertals. J Hum Evol. 2016;90:176-182. doi:10.1016/j.jhevol.2015.09.005.

125. Greenwood DD. A cochlear frequency-position function for several species--29 years later. J Acoust Soc Am. 1990;87(6):2592-2605. doi:10.1121/1.399052.

126. Schurzig D, Timm ME, Batsoulis C, et al. A Novel Method for Clinical Cochlear Duct Length Estimation toward Patient-Specific Cochlear Implant Selection. OTO Open. 2018;2(4):2473974X18800238. doi:10.1177/2473974X18800238.

127. Erixon E, Högstorp H, Wadin K, Rask-Andersen H. Variational anatomy of the human cochlea: implications for cochlear implantation. Otol Neurotol. 2009;30(1):14-22. doi:10.1097/MAO.0b013e31818a08e8.

128. Baskent D, Shannon RV. Speech recognition under conditions of frequency-place compression and expansion. The Journal of the Acoustical Society of America, 113(4), 2064-2076.

129. Ekdale EG. Comparative Anatomy of the Bony Labyrinth (Inner Ear) of Placental Mammals. PLoS One. 2015; 26;10(8):e0137149. doi:10.1371/journal.pone.0066624.

130. Adunka OF, Dillon MT, Adunka MC, King ER, Pillsbury HC, Buchman CA. Cochleostomy versus round window insertions: influence on functional outcomes in electric-acoustic stimulation of the auditory system. Otol Neurotol. 2014;35(4):613-618. doi:10.1097/MAO.0000000000000269.

131. Gani M, Valentini G, Sigrist A, Kós MI, Boëx C. Implications of deep electrode insertion on cochlear implant fitting. J Assoc Res Otolaryngol. 2007;8(1):69-83. doi:10.1007/s10162-006-0065-4.

132. Kalkman RK, Briaire JJ, Dekker DM, Frijns JH. Place pitch versus electrode location in a realistic computational model of the implanted human cochlea. Hear Res. 2014;315:10-24. doi:10.1016/j.heares.2014.06.003.

133. Roy AT, Penninger RT, Pearl MS, et al. Deeper Cochlear Implant Electrode Insertion Angle Improves Detection of Musical Sound Quality Deterioration Related to Bass Frequency Removal. Otol Neurotol. 2016;37(2):146-151. doi:10.1097/MAO.0000000000000932.

134. O'Connell BP, Hunter JB, Gifford RH, et al. Electrode Location and Audiologic Performance After Cochlear Implantation: A Comparative Study Between Nucleus CI422 and CI512 Electrode Arrays. Otol Neurotol. 2016;37(8):1032-1035. doi:10.1097/MAO.0000000000001140.

135. O'Connell BP, Cakir A, Hunter JB, et al. Electrode Location and Angular Insertion Depth Are Predictors of Audiologic Outcomes in Cochlear Implantation. Otol Neurotol. 2016;37(8):1016-1023. doi:10.1097/MAO.0000000000001125.

136. Büchner A, Illg A, Majdani O, Lenarz T. Investigation of the effect of cochlear implant electrode length on speech comprehension in quiet and noise compared with the results with users of electro-acoustic-stimulation, a retrospective analysis. PLoS One. 2017;12(5):e0174900. doi:10.1371/journal.pone.0174900.

137. Stakhovskaya O, Sridhar D, Bonham BH, Leake PA. Frequency map for the human cochlear spiral ganglion: implications for cochlear implants. J Assoc Res Otolaryngol. 2007;8(2):220-233. doi:10.1007/s10162-007-0076-9.

138. Liberman MC. Single-neuron labeling in the cat auditory nerve. Science. 1982;216(4551):1239-1241. doi:10.1126/science.7079757.

139. Falbo C. The golden ratio-A contrary viewpoint. The College Mathematics Journal. 2005;36(2):123-134.

140. Kelley MW. Regulation of cell fate in the sensory epithelia of the inner ear. Nat Rev Neurosci. 2006;7(11):837-849. doi:10.1038/nrn1987.

141. Manoussaki D, Dimitriadis EK, Chadwick RS. Cochlea's graded curvature effect on low frequency waves. Phys Rev Lett. 2006;96(8):088701. doi:10.1103/PhysRevLett.96.088701.

142. Gunz P, Ramsier M, Kuhrig M, Hublin JJ, Spoor F. The mammalian bony labyrinth reconsidered, introducing a comprehensive geometric morphometric approach. J Anat. 2012;220(6):529-543. doi:10.1111/j.1469-7580.2012.01493.x.

143. Coleman MN, Colbert MW. Correlations between auditory structures and hearing sensitivity in non-human primates. J Morphol. 2010;271(5):511-532. doi:10.1002/jmor.10814.

144. Manley GA. Evolutionary paths to mammalian cochleae. J Assoc Res Otolaryngol. 2012;13(6):733-743. doi:10.1007/s10162-012-0349-9.

145. Cantos R, Cole LK, Acampora D, Simeone A, Wu DK. Patterning of the mammalian cochlea. Proc Natl Acad Sci U S A. 2000;97(22):11707-11713. doi:10.1073/pnas.97.22.11707.

146. Dabdoub A, Puligilla C, Jones JM, et al. Sox2 signaling in prosensory domain specification and subsequent hair cell differentiation in the developing cochlea. Proc Natl Acad Sci U S A. 2008;105(47):18396-18401. doi:10.1073/pnas.0808175105.

147. Nishimura T, Hosoi H, Saito O, et al. Effect of fixation place on airborne sound in cartilage conduction. J Acoust Soc Am. 2020;148(2):469. doi:10.1121/10.0001671.

148. Terino EO, Edwards MC. Alloplastic contouring for suborbital, maxillary, zygomatic deficiencies. Facial Plast Surg Clin North Am. 2008;16(1):33-v. doi:10.1016/j.fsc.2007.09.006.

149. Gülekon IN, Turgut HB. The external occipital protuberance: can it be used as a criterion in the determination of sex? J Forensic Sci. 2003;48(3):513-516.

150. Breitsprecher T, Dhanasingh A, Schulze M, et al. CT imaging-based approaches to cochlear duct length estimation-a human temporal bone study. Eur Radiol. 2022;32(2):1014-1023. doi:10.1007/s00330-021-08189-x.

151. Lenarz T, Stover T, Buechner A, et al. Temporal bone results and hearing preservation with a new straight electrode. Audiol Neurootol. 2006;11 Suppl 1:34-41. doi:10.1159/000095612.

152. Lan MY, Shiao JY, Ho CY, Hung HC. Measurements of normal inner ear on computed tomography in children with congenital sensorineural hearing loss. Eur Arch Otorhinolaryngol. 2009;266(9):1361-1364. doi:10.1007/s00405-009-0923-x.

153. Purcell D, Johnson J, Fischbein N, Lalwani AK. Establishment of normative cochlear and vestibular measurements to aid in the diagnosis of inner ear malformations. Otolaryngol Head Neck Surg. 2003;128(1):78-87. doi:10.1067/mhn.2003.51.

154. Pelliccia P, Venail F, Bonafé A, et al. Cochlea size variability and implications in clinical practice. Acta Otorhinolaryngol Ital. 2014;34(1):42-49.

155. Waldeck S, Falck C, Chapot R, Brockmann M, Overhoff D. Determination of Cochlear Duct Length With 3D Versus Two-dimensional Methods: A Retrospective Clinical Study of Imaging by Computed Tomography and Cone Beam Computed Tomography. In Vivo. 2021;35(6):3339-3344. doi:10.21873/invivo.12631.

156. Sato H, Sando I, Takahashi H. Sexual dimorphism and development of the human cochlea. Computer 3-D measurement. Acta Otolaryngol. 1991;111(6):1037-1040. doi:10.3109/00016489109100753.

157. Alanazi A, Alzhrani F. Comparison of cochlear duct length between the Saudi and non-Saudi populations. Ann Saudi Med. 2018;38(2):125-129. doi:10.5144/0256-4947.2018.125.

158. Alnafjan FF, Allan SM, McMahon CM, da Cruz MJ. Assessing Cochlear Length Using Cone Beam Computed Tomography in Adults With Cochlear Implants. Otol Neurotol. 2018;39(9):e757-e764. doi:10.1097/MAO.0000000000001934.

159. Eser MB, Atalay B, Kalcıoğlu MT. Is Cochlear Length Related to Congenital Sensorineural Hearing Loss: Preliminary Data. J Int Adv Otol. 2021;17(1):1-8. doi:10.5152/iao.2020.7863.

160. Takahashi M, Arai Y, Sakuma N, et al. Cochlear volume as a predictive factor for residual-hearing preservation after conventional cochlear implantation. Acta Otolaryngol. 2018;138(4):345-350. doi:10.1080/00016489.2017.1393840.

161. An SY, An CH, Lee KY, Jang JH, Choung YH, Lee SH. Diagnostic role of cone beam computed tomography for the position of straight array. Acta Otolaryngol. 2018;138(4):375-381. doi:10.1080/00016489.2017.1404639.

162. Skinner MW, Ketten DR, Holden LK, et al. CT-derived estimation of cochlear morphology and electrode array position in relation to word recognition in Nucleus-22 recipients. J Assoc Res Otolaryngol. 2002;3(3):332-350. doi:10.1007/s101620020013.

163. Gasser RF. The development of the facial nerve in man. Ann Otol Rhinol Laryngol. 1967;76(1):37-56. doi:10.1177/000348946707600103.

164. Monkhouse WS. The anatomy of the facial nerve. Ear Nose Throat J. 1990;69(10):677-687.

165. Müller F, O'Rahilly R. The human chondrocranium at the end of the embryonic period, proper, with particular reference to the nervous system. Am J Anat. 1980;159(1):33-58. doi:10.1002/aja.1001590105.

166. Gasser RF, Shigihara S, Shimada K. Three-dimensional development of the facial nerve path through the ear region in human embryos. Ann Otol Rhinol Laryngol. 1994;103(5 Pt 1):395-403. doi:10.1177/000348949410300510.

167. Lin YC, Chen CP. Characterization of small-to-medium head-and-face dimensions for developing respirator fit test panels and evaluating fit of filtering facepiece respirators with different faceseal design. PLoS One. 2017;12(11):e0188638. doi:10.1371/journal.pone.0188638.

168. Aoyagi M, Kim Y, Yokoyama J, Kiren T, Suzuki Y, Koike Y. Head size as a basis of gender difference in the latency of the brainstem auditory-evoked response. Audiology. 1990;29(2):107-112. doi:10.3109/00206099009081652.

169. Berman K, Fahri ÖA. Türk Erkek Toplumunun Antropometrik Ölçülerinin Belirlenmesi, ULAKBIM; 1989.

170. Lacko D, Huysmans T, Parizel PM, et al. Evaluation of an anthropometric shape model of the human scalp. Appl Ergon. 2015;48:70-85. doi:10.1016/j.apergo.2014.11.008.

171. Matthews H, Penington T, Saey I, Halliday J, Muggli E, Claes P. Spatially dense morphometrics of craniofacial sexual dimorphism in 1-year-olds. J Anat. 2016;229(4):549-559. doi:10.1111/joa.12507.

172. Grover M, Sharma S, Singh SN, Kataria T, Lakhawat RS, Sharma MP. Measuring cochlear duct length in Asian population: worth giving a thought! Eur Arch Otorhinolaryngol. 2018;275(3):725-728. doi:10.1007/s00405-018-4868-9

173. Singla A, Sahni D, Gupta A. K, Aggarwal A, Gupta T. Surgical anatomy of the basal turn of the human cochlea as pertaining to cochlear implantation. Otology & Neurotology. 2015;36(2):323-328.

174. Atalay B, Eser MB, Kalcıoglu MT. The Length of the Organ of Corti in Humankind: A Meta-Analysis; 2020.

175. Khurayzi T, Almuhawas F, Sanosi A. Direct measurement of cochlear parameters for automatic calculation of the cochlear duct length. Ann Saudi Med. 2020;40(3):212-218. doi:10.5144/0256-4947.2020.218.

176. Rosas A, Ferrando A, Bastir M, et al. Neandertal talus bones from El Sidrón site (Asturias, Spain): A 3D geometric morphometrics analysis. Am J Phys Anthropol. 2017;164(2):394-415. doi:10.1002/ajpa.23280.

177. Arsuaga JL, Martínez I, Arnold LJ, et al. Neandertal roots: Cranial and chronological evidence from Sima de los Huesos. Science. 2014;344(6190):1358-1363. doi:10.1126/science.1253958.

178. Ponce de León MS, Bienvenu T, Akazawa T, Zollikofer CP. Brain development is similar in Neanderthals and modern humans. Curr Biol. 2016;26(14):R665-R666. doi:10.1016/j.cub.2016.06.022.

179. Herculano-Houzel S, Ribeiro P, Campos L, et al. Updated neuronal scaling rules for the brains of Glires (rodents/lagomorphs). Brain Behav Evol. 2011;78(4):302-314. doi:10.1159/000330825.

180. Sakai T, Hirata S, Fuwa K, et al. Fetal brain development in chimpanzees versus humans. Curr Biol. 2012;22(18):R791-R792. doi:10.1016/j.cub.2012.06.062.

8. APPENDIXES

Appendix-1: Non-Interventional Retrospective Clinical Research Ethics Committee's permission.

MHH
Medizinische Hochschule Hannover

Ethikkommission
Vorsitzender:
Prof. Dr. H. D. Tröger

Sekretariat:
Rita Landowski
Telefon: 0511 532-3443
Fax: 0511 532-5423
ethikkommission@mh-hannover.de

Carl-Neuberg-Straße 1
30625 Hannover
Telefon: 0511 532-0
www.mh-hannover.de

MHH Ethikkommission OE 9515
30623 Hannover

Herrn
Prof. Dr. Andreas Büchner
Deutsches Hörzentrum Hannover
Carl-Wiechert-Allee 3 (et cetera Gebäude)
30625 Hannover

09.07.13/La

Veröffentlichung von in der Routine erhobener Daten
Nr. 1897-2013

Sehr geehrter Herr Kollege Büchner,

als Vorsitzender habe ich im Auftrag der Mitglieder der Ethikkommission Ihr Schreiben vom 09.07.13 und die Ausführungen zum o. g. Vorhaben geprüft. Für die Bewertung anonymisierter abteilungsinterner Patientendaten besteht grundsätzlich keine Vorlagepflicht bei der Ethikkommission. Auch aus berufsrechtlicher Sicht bestehen keine ethisch-rechtlichen Bedenken.

Mit besten Grüßen bin ich
Ihr

Prof. Dr. H. D. Tröger
Vorsitzender

Appendix-2: Digital Receipt

turnitin

Dijital Makbuz

Bu makbuz ödevinizin Turnitin'e ulaştığını bildirmektedir. Gönderiminize dair bilgiler şöyledir:

Gönderinizin ilk sayfası aşağıda gönderilmektedir.

Gönderen:	İrem Adalılar
Ödev başlığı:	İrem Adalılar Master Tez
Gönderi Başlığı:	Tez Savunma Sınavı Sonrası
Dosya adı:	CI_LDEDO_NU_S_ECEK.pdf
Dosya boyutu:	13.26M
Sayfa sayısı:	90
Kelime sayısı:	23,136
Karakter sayısı:	121,289
Gönderim Tarihi:	05-May-2022 11:43ÖÖ (UTC+0300)
Gönderim Numarası:	1828825098

Appendix-3: Turnitin Originality Report

Turnitin Orijinallik Raporu

İşleme kondu: 05-May-2022 11:50 +03
NUMARA: 1828825098
Kelime Sayısı: 23136
Gönderildi: 1

Tez Savunma Sınavı Sonrası İrem Adalılar tarafından

Benzerlik Endeksi	Kaynağa göre Benzerlik
%14	Internet Sources: %8 Yayınlar: %11 Öğrenci Ödevleri: %2

1% match (19-Eyl-2020 tarihli internet) https://onlinelibrary.wiley.com/doi/full/10.1111/joa.12308
1% match (13-Şub-2017 tarihli öğrenci ödevleri) Submitted to TechKnowledge Turkey on 2017-02-13
1% match (yayınlar) David M. Landsberger, Maja Svrakic, J. Thomas Roland, Mario Svirsky. "The Relationship Between Insertion Angles, Default Frequency Allocations, and Spiral Ganglion Place Pitch in Cochlear Implants", Ear and Hearing, 2015
< 1% match (04-Haz-2019 tarihli internet) https://onlinelibrary.wiley.com/doi/full/10.1111/joa.12253
< 1% match (29-Eki-2020 tarihli internet) https://onlinelibrary.wiley.com/doi/10.1002/cne.23594
< 1% match (01-Ara-2021 tarihli internet) https://journalotohns.biomedcentral.com/articles/10.1186/s40463-017-0194-2
< 1% match (yayınlar) Würfel, Waldemar, Heinrich Lanfermann, Thomas Lenarz, and Omid Majdani. "Cochlear length determination using Cone Beam Computed Tomography in a clinical setting", Hearing Research, 2014.
< 1% match (04-Kas-2019 tarihli öğrenci ödevleri) Submitted to University of Westminster on 2019-11-04
< 1% match (19-Kas-2021 tarihli internet) https://www.nature.com/articles/s41598-017-07795-4?code=2d87e709-8864-48d3-bf0d-3949d278de92&error=cookies_not_supported
< 1% match (20-Eki-2021 tarihli internet) https://www.nature.com/articles/s41431-020-00739-z?code=1a7c7aa4-3c13-46bc-9274-3b2690fba0c9&error=cookies_not_supported
< 1% match (13-Ağu-2020 tarihli internet) https://www.nature.com/articles/tp2013113?code=60de8fff-23cd-40ca-bace-b84649e21b28&error=cookies_not_supported
< 1% match (yayınlar) Handbook of Anthropometry, 2012.
< 1% match (26-Eki-2014 tarihli internet) http://www.ncbi.nlm.nih.gov/pmc/articles/PMC3400202/
< 1% match (03-May-2020 tarihli internet) https://www.ncbi.nlm.nih.gov/pubmed?Cmd=ShowDetailView&Db=pubmed&TermToSearch=15610391
< 1% match (28-Şub-2020 tarihli internet) https://www.ncbi.nlm.nih.gov/pubmed?Cmd=ShowDetailView&Db=pubmed&TermToSearch=28463804
< 1% match (24-Eki-2010 tarihli internet) http://www.ncbi.nlm.nih.gov/pmc/articles/PMC1571245/
< 1% match (12-Eyl-2017 tarihli internet) https://pdfs.semanticscholar.org/1c9c/794e2658724e5635ef2221c200f04172950c.pdf
< 1% match (07-Ara-2018 tarihli internet) https://pdfs.semanticscholar.org/e490/e992bbcab3c2da89f481c5b0f1a0eff1cbaa.pdf
< 1% match (yayınlar) Basak Atalay, Mehmet Bilgin Eser, Mahmut Tayyar Kalcioglu, Handan Ankarali. "Comprehensive Analysis of Factors Affecting Cochlear Size: A Systematic Review and Meta-analysis", The Laryngoscope, 2021

9. CV

INDIVIDUAL INFORMATION

Name and Surname: İrem Adalılar

Birth Place and Date: Eskişehir / Turkey – 25.05.1998

Nationality: Turkish

EDUCATION

- 2016-2020 Bachelor of Science in Audiology, Hacettepe University
- 2020-2022 Master of Science in Audiology, Hacettepe University, Graduate School of Health Sciences